European Journal of Medicinal Chemistry 96 (2015) 382–395

Contents lists available at ScienceDirect

European Journal of Medicinal Chemistry

journal homepage: http://www.elsevier.com/locate/ejmech

Original article

Synthesis and antitumor activities evaluation of *m*-(4-morpholinoquinazolin-2-yl)benzamides *in vitro* and *in vivo*

Xiao-Meng Wang [a], Min-Hang Xin [a], Jing Xu [b], Bo-Rui Kang [a], Yan Li [a], She-Min Lu [b], San-Qi Zhang [a, *]

[a] Department of Medicinal Chemistry, School of Pharmacy, Xi'an Jiaotong University, Xi'an, Shaanxi 710061, PR China
[b] Department of Genetics and Molecular Biology, School of Basic Medical Sciences, Xi'an Jiaotong University, Xi'an Shaanxi 710061, PR China

ARTICLE INFO

Article history:
Received 16 October 2014
Received in revised form
24 March 2015
Accepted 4 April 2015
Available online 17 April 2015

Keywords:
Benzamide
Quinazoline
Synthesis
Antitumor agents
PI3K inhibitor

ABSTRACT

In the present study, a series of *m*-(4-morpholinoquinazolin-2-yl)benzamides were designed, synthesized and characterized. The antiproliferative activities of the synthesized compounds were evaluated against two human cell lines (HCT-116 and MCF-7). Compounds with IC_{50} values below 4 μM were further evaluated against U-87 MG and A549 cell lines. Among these evaluated compounds, compound **T10** displayed a remarkable antiproliferative effect *in vitro*. The hoechst staining assay showed that compound **T10** caused morphological changes. The cell cycle and apoptosis assay further indicated that compound **T10** can arrest HCT-116 cells in G2/M and G0/G1 phase and induce apoptosis. PI3K enzyme assays indicated that compounds **T7** and **T10** selectively inhibit PI3Kα. A Western bolt assay further suggested that compound **T10** can block the PI3K/Akt/mTOR pathway. Moreover, compound **T10** inhibited tumor growth on a mice S180 homograft model. These findings directly identify *m*-(4-morpholinoquinazolin-2-yl)benzamide derivatives as novel anticancer agents.

1. Introduction

Among heterocyclic systems, the quinazoline ring system has been regarded as a privileged drug scaffold in drug discovery [1]. Quinazoline derivatives exhibit a broad spectrum of biological activities, such as antitumor, anti-inflammatory, antimicrobial and antimalarial activities [2–6]. Moreover, the kinase inhibitors gifitinib, erlotinib and lapatinib that contain a quinazoline core have been approved for the treatment of cancer [7,8]. Recently, AZD8931, a 4,6,7-trisubsituted quinazoline, has been reported as a reversible inhibitor of the EGFR, HER2 and HER3 receptors and thus is a promising drug candidate [9]. A series of novel 4-alkoxyquinazoline derivatives have been reported as potential inhibitors of VEGFR2 [10]. Meanwhile, aminoquinazoline derivatives are described as potent mutant B-Raf ^{V600E} selective inhibitors [11]. 2-Amino-3-substituted quinazolinone derivatives have also been identified as selective inhibitors of PI4KIIIα, which can inhibit HCV replication *in vitro* [12].

PI3K (phosphatidylinositol-3 kinase)/Akt/mTOR (mammalian target of rapamycin) is an important signaling pathway in that it is crucial to diverse cell processes, including cell growth, proliferation, survival, metabolism and autophagy [13–15]. The aberrant activation of PI3K pathway, commonly due to either mutation in PIK3CA gene or loss regulation of PTEN, is closely linked to the development and progression of a wide range of cancers [16,17]. Besides, mTOR, a key node of the PI3K pathway is found to be frequently hyperactivated in human tumors [18]. Therefore, PI3K (especially PI3Kα) and mTOR have emerged as attractive targets for cancer therapy. In recent years, several PI3K inhibitors, such as BKM120 [19], GDC0941 [20], ZSTK474 [21] and NVP-BYL719 [22], have been developed into clinical trials. Additionally, PI3K and mTOR dual inhibitors, such as BEZ235 [23], GSK2126458 [24], GDC0980 [25], PF-04979064 [26] and PKI-587 [27], are also evaluated in clinical trials for their therapeutic potentials. Moreover, the pharmacophore of the PI3K inhibitors has been recently put forward as well [28].

Anticancer candidates BKM120, VS-5584 [29] and GDC0980 possess the similar pharmacophore. The aminopyridinyl group in BKM120, aminopyrimidinyl group in VS-5584 and GDC-0980, and the morpholine in three compounds could form interaction with PI3K. As a PI3K inhibitor, BKM120 exhibited inhibitory activity against PI3Kα with an IC_{50} value of 0.03 μM. The co-crystal

* Corresponding author.
E-mail address: sqzhang@xjtu.edu.cn (S.-Q. Zhang).

http://dx.doi.org/10.1016/j.ejmech.2015.04.037
0223-5234/

structure of BKM120 in PI3Kγ (PDB code 3SD5) indicates that the oxygen atom of a morpholine ring is bound to the hinge at Val882 and the hydrogen atoms from the aminopyridinyl group interact with Asp836 and Asp841 via hydrogen bonds [19]. PI-103 (Fig. 1) is described as a multi-targeted PI3K inhibitor. The crystal structure of the human PI3Kα with PI-103 complex indicates that a substituted group at the *m*-position of the phenol hydroxy of PI-103 may improve its binding affinity by forming a new H-bond [30]. Early, 2-(3-hydroxyphenyl)-4-morpholinoquinazoline and related derivatives were reported as PI3Kα inhibitors [31,32].

Recently, based upon the docking model of GSK2126458 with PI3Kγ [24], we proposed that the water molecule bridge could be replaced by the structure of an amide group. Thereupon, we synthesized a series of 2-substituted-3- phenylsulfonylamino-5-(quinazolin-6-yl or quinolin-6-yl)benzamides and discovered that the designed compounds are novel PI3K inhibitors and anticancer agents [33]. Thereafter, we combined the benzamide moiety with 2-aminobenzothiazole to discover novel anticancer agents [34]. There are two hydrogen bond donors and one hydrogen bond receptor in the structure of benzamide, so the enzymatic inhibitor with a benzamide moiety is east to form interaction with receptor. In this study, we combined benzamide moiety with quinazoline scaffold to design, synthesize and evaluate a series of *m*-(4-morpholinoquinazolin-2-yl)benzamides as antitumor agents (Fig. 2).

2. Results and discussion

2.1. Synthesis

The synthetic route for the title compounds **T1**–**T10** and **T12**–**T21** is outlined in Scheme 1.

2,4-Dichloro-6,7-dialkyloxyquinazoline (**1**) was used as starting material. The reaction of **1** with morpholine produced the key intermediate 2-chloro-4- (4-morpholinyl)-6,7-dialkyloxyquinazoline (**2**). As we previously reported, catalyzed by $PdCl_2$(dppf), the reaction of bis(pinacolato)diboron with substituted bromobenzene **3** yielded phenylboronic ester **4**, which was used for the subsequent Suzuki coupling to produce target compounds **T1**–**T6**, **T9**–**T10**, **T12** and **T14**–**T21** [35]. The preparation of phenylboronic ester and Suzuki coupling was performed in one pot. Compounds **T7** and **T8** with a hydroxy group at either R^5 or R^4 were obtained by debenzylation of compounds **T5** and **T6** with the aid of hydrogenolysis. In addition, the ester group in compound **T12** was hydrolyzed to prepare compound **T13**.

The debenzylation of compound **T21** produced the key intermediate **5**. In the presence of potassium carbonate, the nucleophilic substitution of intermediate **5** with substituted alkyl halide afforded intermediate **6** or target compounds **T22**–**T26**. The ester group in intermediate **6** was hydrolyzed to yield the carboxylic acid **7**, which was subsequently condensed with the corresponding amines to produce target compounds **T27**–**T29** (Scheme 2).

Recently, the 2-(2-aminopyrimidin-5-yl)-4-morpholinylpyridopyrimidine has been reported as a novel PI3K/mTOR dual Inhibitor [36]. To compare the antiproliferative effects of our designed compounds with the analog with an 2-aminopyrimidinyl moiety, compound **T11** was prepared from commercially available 5-bromopyrimidin-2-amine by Suzuki coupling. The synthetic route for compound **T11** is depicted in Scheme 3.

2.2. Biological evaluations

2.2.1. Antiproliferative activities in vitro

The newly synthesized compounds **T1**–**T29** were evaluated by applying the 3-(4,5-Dimethylthiazol-2-yl)-2,5-diphenyltetrazolium bromide (MTT) colorimetric assay for their antiproliferative activities against colon carcinoma cell line (HCT-116) and breast adenocarcinoma carcinoma cell line (MCF-7). The PI3K inhibitor GDC-0941 was used as the positive control. The results expressed as IC_{50} values are summarized in Table 1.

As we expected, all the designed compounds displayed potent antiproliferative activities against the two cancer cell lines. Generally, most of the title compounds were more potent against HCT-116 than they were against MCF-7. Compound **T1** exhibited potent antiproliferative effects against HCT-116 (IC_{50} = 0.90 μM) and MCF-7 (IC_{50} = 2.14 μM). The preliminary results indicate that our design idea is reasonable. The fact that compounds **T2** and **T4** were more potent than compound **T1** against HCT-116 and HCF-7 indicates that the title compound with a methoxy at either R^2 or R^3 may enhance the antiproliferative activity. Moreover, compounds **T5** and **T7** with a substituent at R^3 displayed more potency than compounds **T6** and **T8** with a substituent at R^2, which indicates that a substituent at R^3 position (*m*-position of amide group) may improve antiproliferative activity. Compounds **T5** and **T6** with a benzyloxy gave rise to a decreased potency in comparison with compounds **T4** and **T2**, which suggests that a large substituent such as benzyloxy at *o*-position or *m*-position of the amide group is disadvantageous for antiproliferative activity. In addition, compound **T9** with a trifluoromethyl at R^3 showed a decreased activity compared with compound **T4** as well. However, compound **T10**

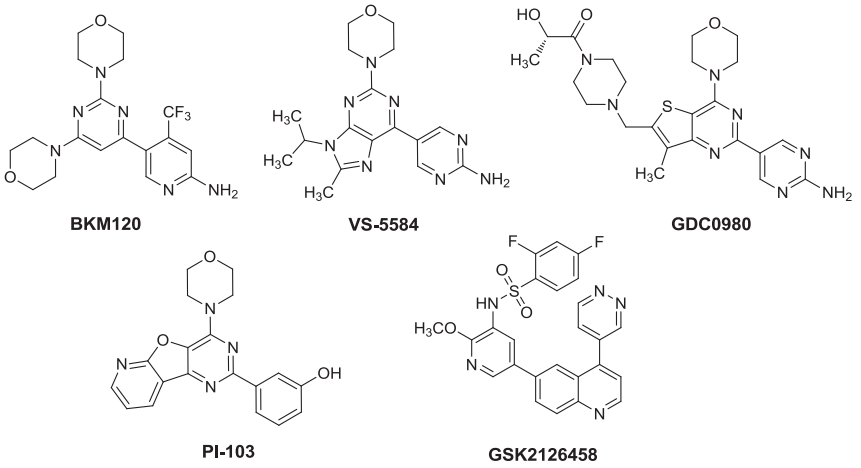

Fig. 1. The structure of several PI3K inhibitors.

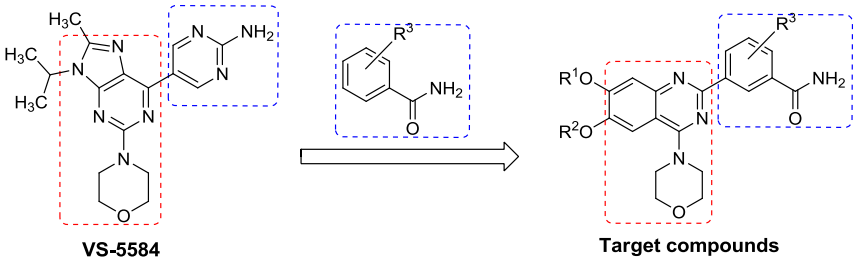

Fig. 2. The design strategy of *m*-(4-morpholinoquinazolin-2-yl)benzamides.

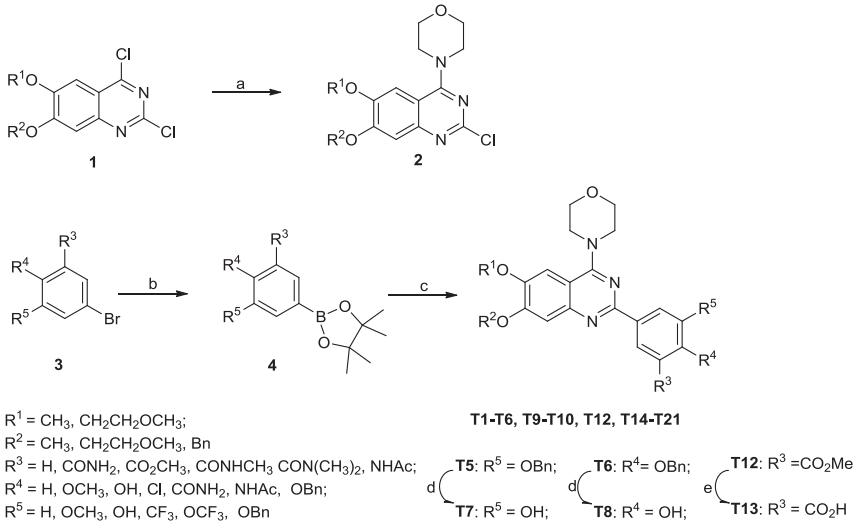

Scheme 1. Synthesis of compounds **T1**–**T8**, **T10**–**T21**. Reagents and conditions: (a) morpholine, Et_3N, THF, 0 °C, 0.5 h, rt, 2 h, 55.8–70.5%; (b) bis(pinacolato)diboron, AcOK, $PdCl_2$(dppf), 1,4-dioxane, reflux, 2 h; (c) **2**, Na_2CO_3, $PdCl_2$(dppf), DME/H_2O (4:1), reflux, 2 h, 43.5–83.2%; (c) Pd/C, HCO_2NH_4, DMF-H_2O (2:1), 100 °C, 6 h, 81.8–84.7%; (d) (c) 2 M NaOH, MeOH–H_2O (4:1), 4 h, 85.4%.

with a trifluoromethoxyl at R^3 exhibited an increased potency in comparison with compound **T4** against the two cancer cell lines. Therefore, a hydrogen-bond receptor at R^3 may help to improve the antiproliferative effect of title compounds.

Compound **T11** with a 2-aminopyrimidinyl moiety exhibited potent antiproliferative activity against two cancer cell lines, but its activity was slightly weaker than compound **T10**. The latter exhibited an excellent antiproliferative activity against HCT-116 (IC_{50} = 0.30 μM) and MCF-7 (IC_{50} = 1.09 μM), which is almost similar to the positive control GDC0941 (IC_{50} = 0.37 μM against HCT-116; IC_{50} = 1.09 μM against MCF-7). The above results suggest that a trifluoromethoxy at R^3 is the most favorable substituent for

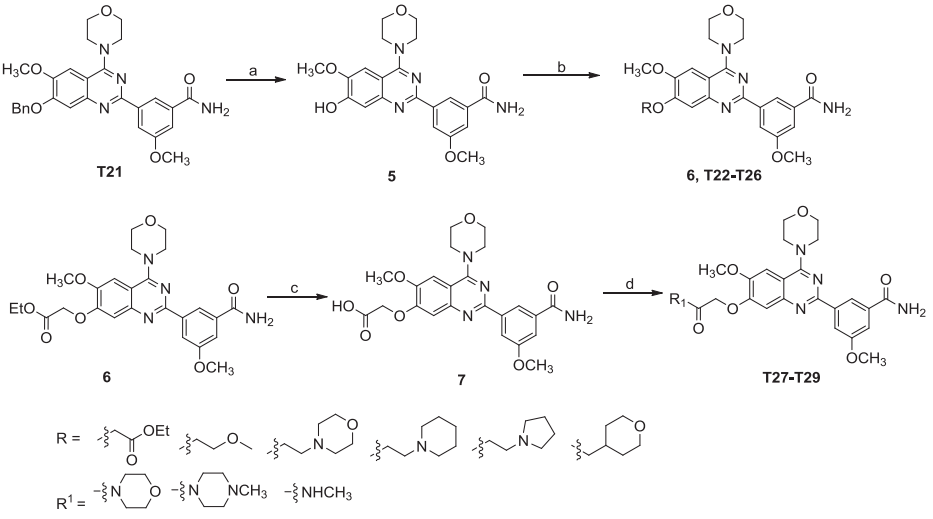

Scheme 2. Synthesis of compounds **T22**–**T27**. Reagents and conditions: (a) Pd/C, HCO_2NH_4, DMF–H_2O (2:1), 100 °C, 6 h, 84.5%; (b) RX, K_2CO_3, KI, DMF, 90 °C, 5–8 h, 63.1–85.2%; (c) 2 M NaOH, MeOH–H_2O (4:1), 4 h, 71.2%; (d) R^1H, EDCI, HOBt, DMF, 8 h, 49.5–75.4%.

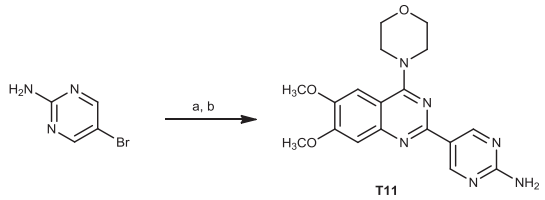

Scheme 3. Synthesis of compound **T11**. Reagents and conditions: (a) bis(pinacolato) diboron, AcOK, $PdCl_2$(dppf), 1,4-dioxane, reflux, 2 h; (b) intermediate **2**, Na_2CO_3, $PdCl_2$(dppf), DME/H_2O (4: 1), reflux, 2 h, 67.8%.

benzamide moiety.

To probe the structure-activity relationship (SAR) of title compounds, the amide group in **T1** was replaced by ester, carboxyl, *N*-methylamide, *N*, *N*-dimethylamide or acetylamino group to obtain compounds **T12**–**T16**. As we expected, the antiproliferative effects of compounds **T12**–**T16** were not improved in comparison with compound **T1**. Thereafter, Moving the amide or acetamino substituent from R^1 position to R^2 position obtained compounds **T17** and **T18**, which displayed a decline in activity. These results supported our design idea that the formamide moiety at *m*-position is important to the maintenance of the antiproliferative activities. Therefore, we argue that the benzamide moiety is part of pharmacophore in the structure of title compounds.

To further improve the solubility and antiproliferative potency of the title compounds, we replaced the methoxy at 6- or 7-positions of the quinazoline ring with the substituents bearing more saturated carbon atoms (Table 2). Table 2 shows that only compound **T26** displayed increased activities against MCF-7 (IC_{50} = 1.01 μM), which is similar to **T4** and **GDC0941** whereas other compounds exhibited decreased potency in comparison with compound **T4**. Therefore, the methoxy at 6- or 7-positions of the quinazoline ring is a suitable group for maintaining antiproliferative activity.

The compounds with IC_{50} values below 4 μM against both HCT-116 and MCF-7 were further evaluated against glioma cell line (U-87 MG) and lung adenocarcinoma epithelial cell line (A549). As shown in Table 3, all the compounds displayed more potency against U-87 MG than against A549. Moreover, compound **T10** exhibited excellent antiproliferative activity against both U-87 MG (IC_{50} = 0.60 μM) and A549 (IC_{50} = 1.68 μM). The results further verify that a trifluoromethoxy at the *m*-position of amide group is

Table 1
Antiproliferative activities of compounds **T1**–**T18** ($\bar{x}\pm s$, n = 3).

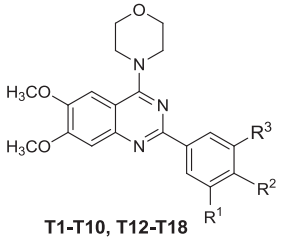

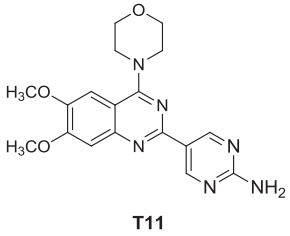

Compds	R^1	R^2	R^3	IC_{50} (μM)	
				HCT-116	MCF-7
T1	$CONH_2$	H	H	0.90 ± 0.15	2.14 ± 0.21
T2	$CONH_2$	OCH_3	H	0.47 ± 0.15	1.22 ± 0.21
T3	$CONH_2$	Cl	H	2.97 ± 0.58	4.24 ± 0.72
T4	$CONH_2$	H	OCH_3	0.45 ± 0.06	1.75 ± 0.32
T5	$CONH_2$	H	OBn	3.83 ± 0.35	6.93 ± 0.75
T6	$CONH_2$	OBn	H	5.03 ± 0.49	7.90 ± 0.40
T7	$CONH_2$	H	OH	0.88 ± 0.23	2.64 ± 0.46
T8	$CONH_2$	OH	H	2.77 ± 0.46	7.42 ± 1.51
T9	$CONH_2$	H	CF_3	0.71 ± 0.09	2.03 ± 0.20
T10	$CONH_2$	H	OCF_3	0.30 ± 0.06	1.09 ± 0.25
T11				0.42 ± 0.06	1.38 ± 0.39
T12	CO_2CH_3	H	H	1.07 ± 0.16	3.44 ± 0.76
T13	CO_2H	H	H	12.50 ± 2.69	>20
T14	$CONHCH_3$	H	H	2.52 ± 1.04	6.20 ± 0.63
T15	$CON(CH_3)_2$	H	H	4.73 ± 0.68	5.01 ± 0.12
T16	NHAc	H	H	1.42 ± 0.32	3.49 ± 0.57
T17	H	$CONH_2$	H	1.25 ± 0.06	4.60 ± 0.95
T18	H	NHAc	H	1.09 ± 0.09	3.61 ± 0.84
GDC0941				0.37 ± 0.06	1.09 ± 0.15

Table 2
Antiproliferative activities of compounds **T19**–**T29** ($\bar{x}\pm s$, n = 3).

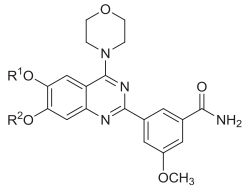

Compds	R^1	R^2	IC_{50} (μM)	
			HCT-116	MCF-7
T4	CH_3	CH_3	0.45 ± 0.15	1.75 ± 0.32
T19	$CH_2CH_2OCH_3$	CH_3	0.89 ± 0.11	5.19 ± 1.32
T20	$CH_2CH_2OCH_3$	$CH_2CH_2OCH_3$	9.04 ± 0.16	7.52 ± 2.51
T21	CH_3	Bn	6.45 ± 1.67	10.27 ± 2.75
T22	CH_3	$CH_2CH_2OCH_3$	2.70 ± 0.56	>20
T23	CH_3		3.14 ± 0.52	8.52 ± 2.42
T24	CH_3	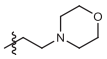	4.72 ± 0.49	5.66 ± 2.41
T25	CH_3	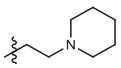	1.28 ± 0.29	6.38 ± 0.98
T26	CH_3	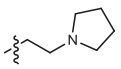	0.81 ± 0.33	1.01 ± 0.30
T27	CH_3	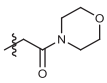	6.48 ± 0.47	24.38 ± 7.13
T28	CH_3	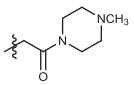	9.44 ± 0.67	18.74 ± 5.14
T29	CH_3	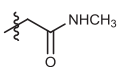	21.68 ± 7.35	14.90 ± 2.24
GDC0941			0.37 ± 0.06	1.09 ± 0.15

Table 3
Antiproliferative activity of chosen compounds ($\bar{x}\pm s$, n = 3).

Compds	IC_{50} (μM)	
	U-87 MG	A549
T1	1.57 ± 0.05	26.10 ± 1.80
T2	1.90 ± 0.17	9.63 ± 0.33
T4	1.01 ± 0.21	9.22 ± 0.55
T7	1.84 ± 0.48	17.18 ± 2.45
T9	1.19 ± 0.15	4.75 ± 1.28
T10	0.60 ± 0.08	1.68 ± 0.29
T11	5.00 ± 1.35	3.21 ± 0.17
T26	2.45 ± 0.22	9.37 ± 0.41
GDC0941	1.24 ± 0.22	2.28 ± 0.05

advantageous for antiproliferative activity.

From the data in Tables 1–3, we can conclude that the benzamide moiety is important to the maintenance of the antiproliferative activity of title compounds. What's more, a trifluoromethoxy or methoxy or hydroxyl group at *m*-position of amide group and methoxy at 6- and 7-positions of the quinazoline ring are favorable for antiproliferative activity. On account of the antiproliferative activities of compound **T10** are close to those of **GDC0941**, compound **T10** was selected for further investigation.

2.2.2. The effect of compound T10 on cellular morphology

In the present study, the effect of compound **T10** on cellular morphological changes was also investigated. HCT-116 cells were selected and treated with compound **T10** at the concentrations of 0.1 μM, 1 μM and 10 μM for 24 h. The cells were first examined directly and then photographed under a phase contrast microscope followed by stained with Hoechst 33258. As shown in Fig. 3A, the cellular morphological changes such as cell shrinking, vacuolization and fragmentation were observed at 1 μM and 10 μM. The images in Fig. 3B indicated that compound **T10** induced chromatin condensation and nuclear fragmentation. These results suggested that compound **T10** could significantly inhibit cell growth and induce apoptosis accompanying cellular morphological changes.

2.2.3. The effect of compound T10 on cell cycle

To further understand the mechanism of the antiproliferative activity of compound **T10**, the effect of compound **T10** on cell cycle distribution was studied. HCT-116 cells were treated with 3 μM of compound **T10** for 24 h and then stained with propidium iodide (PI). DNA contents were measured by flow cytometry and the results were shown in Fig. 4. The control group treated with DMSO had approximately 48.31% in the G0/G1 phase, 38.71% in the S phase and 12.98% in the G2/M phase. After treated with compound **T10**, the cells in the G0/G1 and G2/M phase increased to 56.69% and 23.19%, respectively and the cells in the S phase decreased to 20.11%. These results indicated that compound **T10** can induce a cell arrest at G2/M and G0/G1 phase.

2.2.4. The effect of compound T10 on apoptosis

To characterize whether compound **T10** induces cell apoptosis, the annexin-V/propidium iodide (PI) biparametric cytofluorimetric assay was performed on HCT-116 cells. The cells were treated with DMSO and compound **T10** at 1 μM and 3 μM for 24 h. As shown in Fig. 5, the percentages of apoptotic cells are 22.70% and 27.34% at 1 μM and 3 μM for compound **T10**, respectively, which is higher than control group. The results indicated that compound **T10** can induce the apoptosis of HCT-116 cells.

2.2.5. PI3K enzymatic activity assay

To elucidate the mechanism of antiproliferative activity of title compounds, **T7** and **T10** were chosen to measure inhibitory enzymatic activity against PI3Ks *in vitro*. An ATP depletion assay was performed preliminarily with **GDC0941** as positive control [19]. The results presented as IC_{50} are summarized in Table 4. As the data in Table 4, compound **T7** could selectively inhibit PI3Kα and **T10** could inhibit both PI3Kα and PI3Kβ, but both **T7** and **T10** displayed weaker activity than that of **GDC0941**. These results suggested that compounds **T7** and **T10** are potential PI3K inhibitors.

It was reported that 2-(3-hydroxyphenyl)-4-morpholinoquinazoline is a PI3Kα inhibitor, but its activity against A375 cell was weak [31]. Generally, the compound with a hydroxyl at phenyl ring is a weak spot in metabolism. Compound **T7** with a phenolic hydroxyl group exhibited higher activity than **T10** against PI3Kα, but displayed weaker activity than **T10** in cell-based activity. The change may relate to the difference of cell penetration ability between **T7** and **T10**. In this work, the hydroxyl at phenyl ring was successfully replaced by the carboxamide moiety, which is a significant structural optimization.

2.2.6. The effect on PI3K/Akt/mTOR pathway

To further verify the mechanism of the antiproliferative activity of compound **T10**, Western blot assay was employed to evaluate the blocking activity of compound **T10** against PI3K/Akt/mTOR pathway. HCT-116 cells were treated with compound **T10** and **GDC0941**, respectively, at a concentration of 10 μM. Meanwhile, the control group was treated with vehicle (0.5% DMSO), whose results are shown in Fig. 6. Compared with the control, both compound **T10** and **GDC0941** could reduce the amount of phosphorylated Akt at Ser-473 without affecting Akt as a whole, but the inhibitory activity of compound **T10** was weaker than that of GDC0941. All this suggested that compound **T10** can block the PI3K/Akt/mTOR pathway, and thus might be a potential PI3K inhibitor.

2.2.7. Anticancer effect on the mice S180 homograft models in vivo

Last, we tested the anticancer effect of compound **T10** on the homograft mice models established for this study. Mice bearing

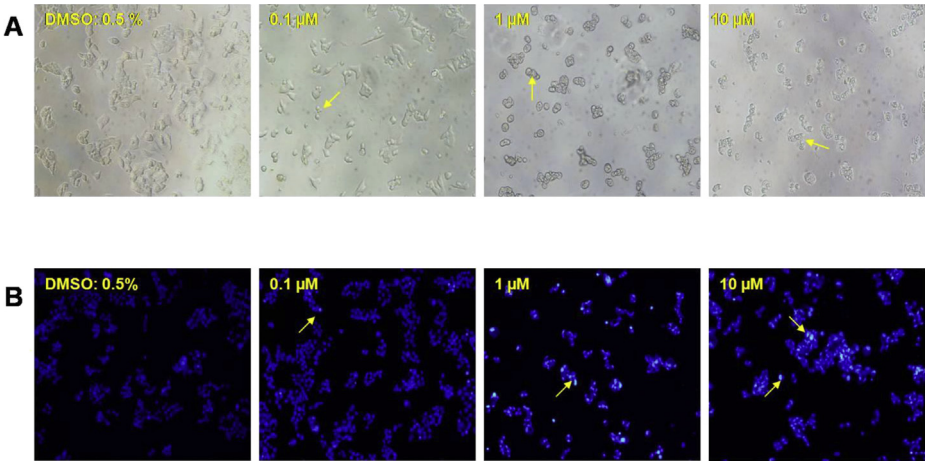

Fig. 3. The effect of compound **T10** on cellular morphology and apoptosis. The HCT-116 cells were treated with compound **T10** at 0.1, 1 and 10 μM. (A) The phase-contrast microscopic view. The yellow arrows indicate the morphological changes of HCT-116. Scale bar = 1.0 mm. (B) The fluorescence microscopic view. The yellow arrows indicate apoptotic cells. Scale bar = 1.0 mm. (For interpretation of the references to colour in this figure legend, the reader is referred to the web version of this article.)

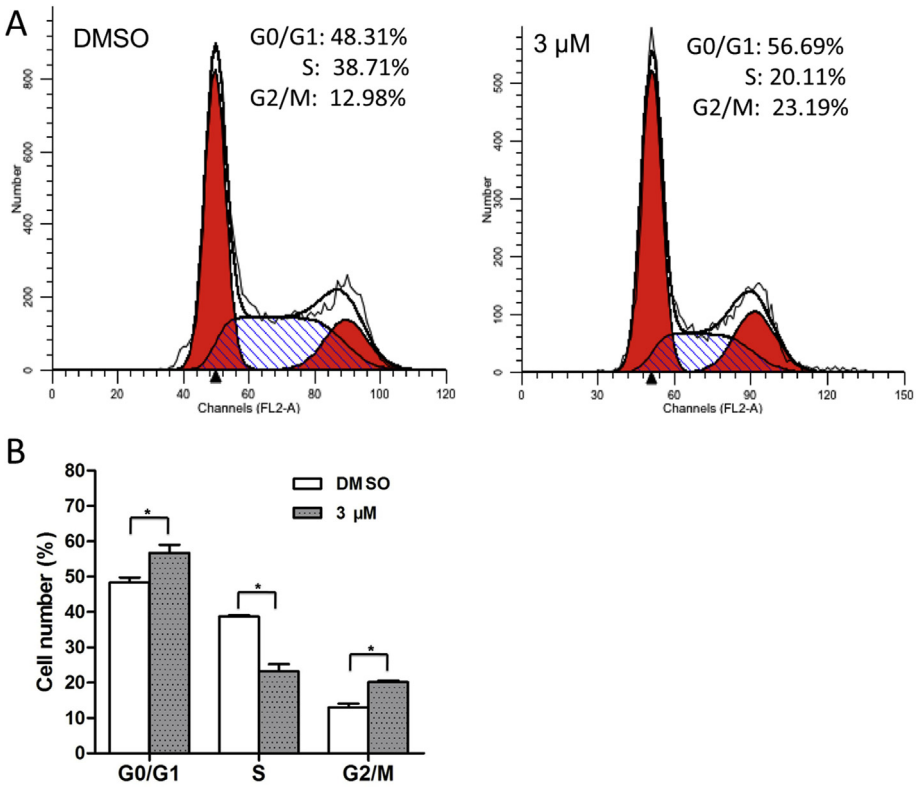

Fig. 4. Effect of compound **T10** on the cell cycle distribution of HCT-116 cells. (A) HCT-116 cells were treated with DMSO or 3 μM of compound **T10** for 24 h. Result presented is an average value of three independent experiments. (B) Quantitative analysis of cell cycle distribution of HCT-116 cells by flow cytometry. Data are the means ± SD of values from three independent experiments (*$p < 0.05$).

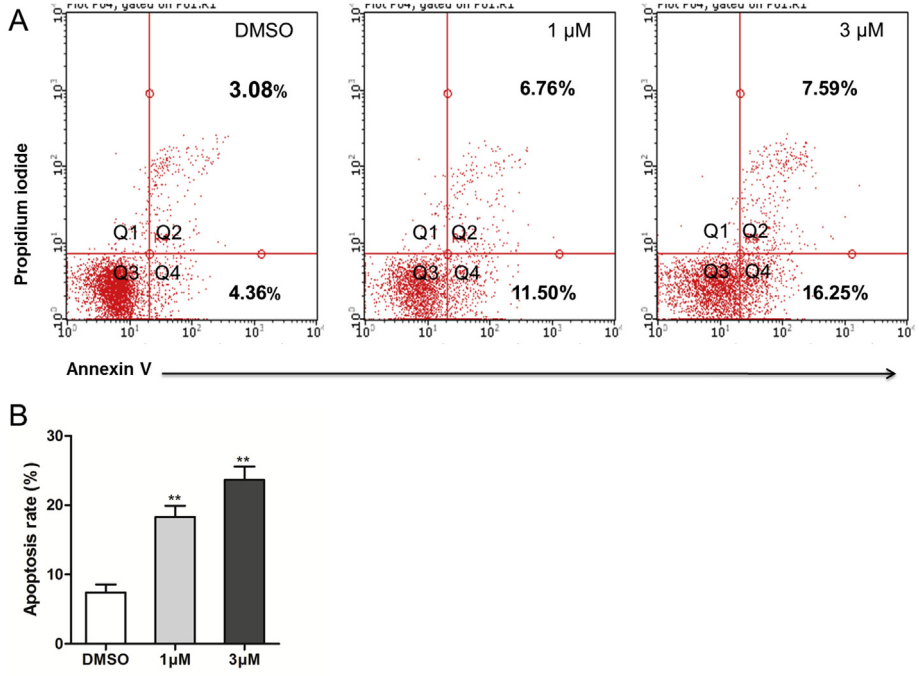

Fig. 5. The effect of compound **T10** on apoptosis. (A) After treated with DMSO, 1 and 3 μM of compound **T10** for 24 h, the HCT-116 cells were harvested, stained with Annexin V and propidium iodide (PI) and analyzed by flow cytometry. The upper left quadrant Q1 represented necrotic cells, the upper right quadrant Q2 represented for late apoptotic cells, the low left quadrant Q3 represented live cells and the low right quadrant Q4 represented for early apoptotic cells. Result presented is a representative of three independent experiments. (B) The apoptosis rate was the sum of Q2 + Q4. Data are the means ± SD of values from three independent experiments (**$p < 0.01$).

Table 4
Enzymatic activity of **T7** and **T10** (IC_{50}, nM, n = 2).

Kinase	T7	T10	GDC0941
PI3Kα	53	96	18
PI3Kβ	454	128	108
PI3Kγ	394	465	117
PI3Kδ	260	330	163

sarcoma (S180) were treated orally with compound **T10** at 15 mg/kg or 30 mg/kg once a day for 8 days. As it was difficult to measure the volume of S180 tumor, tumor weights were used as evaluating indicators illustrated in Fig. 7. The inhibitory ratios of compound **T10** at 15 mg/kg and 30 mg/kg were 49.3% and 64.2%, respectively. Additionally, it was found that compound **T10** had hardly any effect on the body weights of the tested mice. These results suggested that **T10** can significantly inhibit tumor growth *in vivo* and be an effective anticancer agent.

2.3. Molecular docking studies

To explore the binding mode of **T7** and **T10** with PI3Kγ, the C-DOCKER program within Discovery Studio 2.5 software package was utilized to dock **T7** and **T10** with human PI3Kγ (PDB code 3R7R) [37] and the results were depicted in Fig. 8. By the analysis of the binding mode of **T7** and **T10** with PI3Kγ, we observed that the oxygen in morpholine ring formed a hydrogen bond with Val882, one hydrogen atom in amide moiety interacted with Ala 885 and the 7-methoxy of quinazoline formed a hydrogen bond with Lys833, which further verified that the amide group at phenyl ring and 7-methoxy are suitable groups to maintain the activity. In addition, the hydroxyl of **T7** can form a hydrogen bond with Thr887, while one fluorine atom in **T10** formed a hydrogen bond with Lys890.

3. Conclusions

In the present study, title compounds were designed, synthesized and characterized and their antiproliferative activities against HCT-116 and MCF-7 cancer cell lines were evaluated. Most of the compounds exhibited potent antiproliferative activity. The SAR of the title compounds reveals that the benzamide moiety is important to the maintenance of the antiproliferative activity of the title compounds. Besides, a trifluoromethoxy at *m*-position of the amide group and methoxy at 6- and 7-positions of the quinazoline ring are also favorable substituents. Compound **T10** displayed a remarkable antiproliferative activity, and can induce apoptosis at 1 μM and 3 μM. The PI3K enzymatic activity assay and Western blot assay suggested that compound **T10** can block the PI3K/AKT/mTOR pathway. Furthermore, compound **T10** can suppress tumor growth on the mice bearing the sarcoma S180 model. These findings strongly support our assumptions that the title compounds are novel anticancer agents.

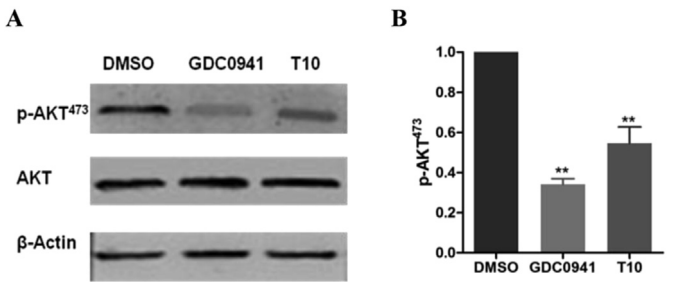

Fig. 6. The effect of compound **T10** on the expression of PI3K/AKT/mTOR pathway of HCT-116 cells at 10 μM. (A) Effect of compounds **T10** and GDC0941 on the expression of p-AKT at Ser-473 and total AKT. (B) The quantified effect of compounds **T10** and GDC0941 on the expression of p-AKT at Ser-473 and total AKT. Each experiment was in triplicate and independently performed. The results were shown as means ± SD. **P < 0.01.

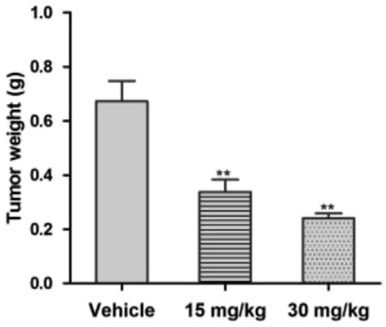

Fig. 7. The antitumor effect of compound **T10** on S180 homograft model. Mice bearing subcutaneous tumors were orally administered vehicle, compound **T10** (15 mg/kg or 30 mg/kg doses) once daily for 8 days. **P < 0.01.

4. Experimental protocols

4.1. Chemistry and chemical methods

Unless specified otherwise, all the starting materials, reagents and solvents were commercially available. All the reactions were monitored by thin-layer chromatography on silica gel plates (GF-254) and visualized with UV light. All the melting points were determined on a micro melting-point apparatus (Beijing) and thermometer was uncorrected. NMR spectra were recorded on a 400 Bruker NMR spectrometer with tetramethylsilane (TMS) as an internal reference. All the chemical shifts are reported in parts per million (ppm). Mass spectra were recorded on a triple quadrupole LC/MS/MS (API 3200, AB SCIEX). HRMS measurements were performed using electrospray ionization (positive mode) on a quadrupole time-of-flight (QTOF) mass spectrometer (Maxis Q-TOF, Bruker Inc.).

4.1.1. General procedure for the synthesis of compound ***2***

To the mixture of 2,4-dichloro-6,7-dialkyloxyquinazoline **1** (10 mmol) and DIPEA (3.49 mL, 20 mmol) in 20 mL of THF was added morpholine (0.88 mL, 10 mmol) dropwise at 0 °C. The mixture was stirred at 0 °C for 0.5 h and then stirred at room temperature for 2 h. The solvent was evaporated to give a residue. To the residue was added the mixture of ethanol and water (40 mL, 1:1) and stirred at room temperature for 0.5 h. The precipitate was filtered, washed by ethanol and water and dried to afford compound **2**.

*4.1.1.1. 4-(2-Chloro-6,7-dimethoxyquinazolin-4-yl)morpholine (**2a**).* Pale yellow solid; Yield 70.5%; mp 213–214 °C; ^{1}H NMR ($CDCl_3$): δ 7.25 (s, 1H, Ar–H), 7.06 (s, 1H, Ar–H), 7.58 (d, J = 8.8 Hz, 1H, Ar–H), 4.02 (s, 3H, OCH_3), 4.00 (s, 3H, OCH_3), 3.91 (m, 4H, $CH_2 \times 2$), 3.79 (m, 4H, $CH_2 \times 2$).

*4.1.1.2. 4-(2-Chloro-6,7-Bis(2-methoxyethoxy)quinazolin-4-yl)morpholine (**2b**).* White solid; Yield 55.8%; mp 94–95 °C; ^{1}H NMR ($CDCl_3$): δ 7.23 (s, 1H, Ar–H), 7.19 (s, 1H, Ar–H), 7.58 (d, J = 8.8 Hz, 1H, Ar–H), 4.27 (m, 4H, $CH_2 \times 2$), 3.91 (m, 8H, $CH_2 \times 4$), 3.76 (m, 4H, $CH_2 \times 2$), 3.48 (d, J = 1.6 Hz, 6H, $CH_3 \times 2$). MS (ESI, m/z): 400.1 $[M + H]^+$.

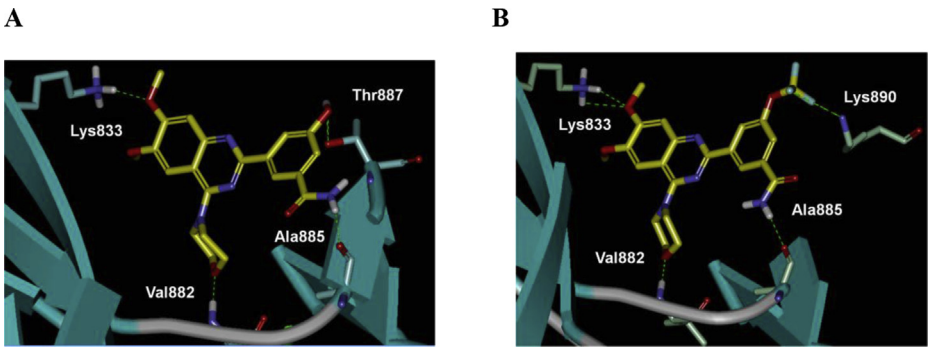

Fig. 8. Docking model of compounds **T7** and **T10** with PI3Kγ. **A**: The docking mode of **T7** with PI3Kγ; **B**: The docking mode of **T10** with PI3Kγ; Selected residues Lys833, Val882, Ala 885, Thr887 and Lys890 are shown. Green dashed lines indicate hydrogen bond. (For interpretation of the references to colour in this figure legend, the reader is referred to the web version of this article.)

*4.1.1.3. 4-(2-Chloro-7-methoxy-6-(2-methoxyethoxy)quinazolin-4-yl)morpholine (**2c**).* Off-white solid; Yield 62.9%; mp 112–114 °C; ^{1}H NMR ($CDCl_3$): δ 7.22 (s, 1H, Ar–H), 7.20 (s, 1H, Ar–H), 7.58 (d, J = 8.8 Hz, 1H, Ar–H), 4.28 (m, 2H, CH_2), 4.00 (s, 3H, OCH_3), 3.90 (m, 4H, $CH_2 \times 2$), 3.86 (m, 2H, CH_2), 3.77 (m, 4H, $CH_2 \times 2$), 3.48 (s, 3H, OCH_3). MS (ESI, m/z): 354.1 $[M + H]^+$.

*4.1.1.4. 4-(7-(Benzyloxy)-2-Chloro-6-methoxyquinazolin-4-yl)morpholine (**2d**).* White solid; Yield 57.4%; mp 168–170 °C; ^{1}H NMR (DMSO-d_6): δ 7.50 (d, J = 7.2 Hz, 2H, Ar–H × 2), 7.43 (m, 2H, Ar–H × 2), 7.37 (m, 1H, Ar–H), 7.30 (s, 1H, Ar–H), 7.17 (s, 1H, Ar–H), 5.29 (s, 2H, OCH_2), 3.92 (s, 3H, OCH_3), 3.76 (m, 8H, $CH_2 \times 4$). MS (ESI, m/z): 386.1 $(M + H)^+$.

*4.1.2. General procedure for the synthesis of compounds **T1**–**T6**, **T9**–**T10**, **T12** and **T14**–**T21***

A mixture of substituted 3-(or 4-) bromobenzamides or 3-bromobenzoate or *N*-(3-(or 4-)bromophenyl)acetamide **3**, (0.5 mmol), bis(pinacolato)diboron (0.14 g, 0.55 mmol), potassium acetate (0.15 g, 1.5 mmol), $PdCl_2$(dppf) (0.03 g, 0.04 mmol) and 1,4-dioxane (10 mL) was refluxed for 2 h under nitrogen atmosphere. The solvent was evaporated under reduced pressure to afford a dark brown residue. To the residue was added intermediate **2** (0.4 mmol), sodium carbonate (0.16 g, 1.5 mmol), $PdCl_2$(dppf) (0.03 g, 0.04 mmol), 1,2-dimethoxyethane (8 mL) and water (2 mL) and the mixture was refluxed for 2 h under nitrogen atmosphere. The mixture was evaporated under reduced pressure and purified by silica gel column chromatography using chloroform/methanol = 30: 1 as the eluent to afford the compounds **T1**–**T6**, **T9**–**T10**, **T12** and **T14**–**T21** as an off-white or a white solid.

*4.1.2.1. 3-(6,7-Dimethoxy-4-morpholinoquinazolin-2-yl)benzamide (**T1**).* White solid; Yield 55.3%; mp 244–246 °C; ^{1}H NMR (DMSO-d_6): δ 8.95 (s, 1H, Ar–H), 8.59 (d, J = 7.6 Hz, 1H, Ar–H), 8.12 (s, 1H, CONH), 7.97 (d, J = 7.6 Hz, 1H, Ar–H), 7.58 (m, 1H, Ar–H), 7.46 (s, 1H, CONH), 7.38 (s, 1H, Ar–H), 7.20 (s, 1H, Ar–H), 3.98 (s, 3H, OCH_3), 3.95 (s, 3H, OCH_3), 3.86 (m, 4H, $CH_2 \times 2$), 3.74 (s, 4H, $CH_2 \times 2$). ^{13}C NMR (DMSO-d_6): δ 168.5 (Cq), 163.8 (Cq), 157.0 (Cq), 155.0 (Cq), 149.6 (Cq), 148.7 (Cq) 138.9 (Cq), 135.1 (Cq), 130.7 (CH), 129.1 (CH), 128.7 (CH), 127.5 (CH), 109.8 (Cq), 108.0 (CH), 103.8 (CH), 66.5 ($CH_2 \times 2$), 56.4 (CH_3), 56.1 (CH_3), 50.3 ($CH_2 \times 2$). MS (ESI, m/z): 395.1 $[M + H]^+$. ESI-HRMS m/z: calc'd for $C_{21}H_{23}N_4O_4$ $[M + H]^+$: 395.1719; found 395.1714.

*4.1.2.2. 5-(6,7-Dimethoxy-4-morpholinoquinazolin-2-yl)-2-methoxybenzamide (**T2**).* White solid; Yield 73.3%; mp 223–225 °C; ^{1}H NMR (DMSO-d_6): δ 8.92 (d, J = 2.4 Hz, 1H, Ar–H), 8.54 (dd, J_1 = 8.8 Hz, J_2 = 2.4 Hz, 1H, Ar–H), 7.71 (s, 1H, CONH), 7.61 (s, 1H, CONH), 7.35 (s, 1H, Ar–H), 7.26 (d, J = 8.8 Hz, 1H, Ar–H), 7.17 (s, 1H, Ar–H), 3.97 (s, 3H, OCH_3), 3.94 (s, 3H, OCH_3) 3.93 (s, 3H, OCH_3), 3.87 (m, 4H, $CH_2 \times 2$), 3.70 (s, 4H, $CH_2 \times 2$). ^{13}C NMR (DMSO-d_6): δ 166.8 (Cq), 163.8 (Cq), 159.1 (Cq), 156.9 (Cq), 154.9 (Cq), 149.7 (Cq), 148.4 (Cq), 132.1 (CH), 131.1 (Cq), 130.8 (Cq), 123.2 (CH), 112.3 (CH), 109.5 (Cq), 108.1 (CH), 103.8 (CH), 66.5 ($CH_2 \times 2$), 56.5 (CH_3), 56.4 (CH_3), 56.1 (CH_3), 50.3 ($CH_2 \times 2$). MS (ESI, m/z): 425.1 $[M + H]^+$. ESI-HRMS m/z: calc'd for $C_{22}H_{24}N_4O_5$ $[M + H]^+$: 425.1825; found 425.1822.

*4.1.2.3. 2-Chloro-5-(6,7-Dimethoxy-4-morpholinoquinazolin-2-yl) benzamide (**T3**).* White solid; Yield 56.0%; mp > 250 °C; ^{1}H NMR (DMSO-d_6): δ 8.49 (s, 1H, Ar–H), 8.47 (d, J = 8.4 Hz, 1H, Ar–H), 8.03 (s, 1H, CONH), 7.70 (s, 1H, CONH), 7.62 (d, J = 8.4 Hz, 1H, Ar–H), 7.36 (s, 1H, Ar–H), 7.18 (s, 1H, Ar–H), 3.97 (s, 3H, OCH_3), 3.94 (s, 3H, OCH_3), 3.86 (d, J = 4.0 Hz, 4H, $CH_2 \times 2$), 3.72 (d, J = 4.0 Hz, 4H, $CH_2 \times 2$). ^{13}C NMR (DMSO-d_6): δ 168.7 (Cq), 163.8 (Cq), 155.9 (Cq), 155.0 (Cq), 149.5 (Cq), 148.8 (Cq), 137.7 (Cq), 137.5 (Cq), 131.6 (CH), 130.2 (CH), 129.7 (CH), 127.9 (Cq), 109.8 (Cq), 108.1 (CH), 103.8 (CH), 66.4 ($CH_2 \times 2$), 56.4 (CH_3), 56.2 (CH_3), 50.2 ($CH_2 \times 2$). MS (ESI, m/z): 411.1 $[M + H]^+$. ESI-HRMS m/z: calc'd for $C_{22}H_{22}ClN_4O_4$ $[M + H]^+$: 429.1330; found 429.1324.

*4.1.2.4. 3-methoxy-5-(6,7-dimethoxy-4-morpholinoquinazolin-2-yl) benzamide (**T4**).* White solid; Yield 60.3%; mp 238–240 °C; ^{1}H NMR (DMSO-d_6): δ 8.49 (s, 1H, Ar–H), 8.47 (d, J = 8.4 Hz, 1H, Ar–H), 8.03 (s, 1H, CONH), 7.70 (s, 1H, CONH), 7.62 (d, J = 8.4 Hz, 1H, Ar–H), 7.36 (s, 1H, Ar–H), 7.18 (s, 1H, Ar–H), 3.97 (s, 3H, OCH_3), 3.94 (s, 3H, OCH_3), 3.86 (d, J = 4.0 Hz, 4H, $CH_2 \times 2$), 3.72 (d, J = 4.0 Hz, 4H, $CH_2 \times 2$). ^{13}C NMR (DMSO-d_6): δ 168.3 (Cq), 163.8 (Cq), 159.7 (Cq), 156.8 (Cq), 155.0 (Cq), 149.6 (Cq), 148.8 (Cq), 140.3 (Cq), 136.4 (Cq), 120.0 (CH), 116.2 (CH), 114.5 (CH), 109.8 (Cq), 108.1 (CH), 103.8 (CH), 66.5 ($CH_2 \times 2$), 56.4 (CH_3), 56.1 (CH_3), 55.9 (CH_3), 50.3 ($CH_2 \times 2$). MS (ESI, m/z): 429.1 $[M + H]^+$. ESI-HRMS m/z: calc'd for $C_{22}H_{24}N_4O_5$ $[M + H]^+$: 425.1825; found 425.1819.

*4.1.2.5. 3-(benzyloxy)-5-(6,7-dimethoxy-4-morpholinoquinazolin-2-yl)benzamide (**T5**).* White solid; Yield 77.4%; mp 165–166 °C; ^{1}H NMR (DMSO-d_6): δ 8.50 (s, 1H, Ar–H), 8.18 (s, 1H, CONH), 8.11 (s, 1H, CONH), 7.64 (m, 1H, Ar–H), 7.53 (d, J = 7.2 Hz, 2H, Ar–H, CONH), 7.44 (m, 3H, Ar–H × 3), 7.37 (m, 2H, Ar–H × 2), 7.18 (s, 1H, Ar–H), 5.29 (s, 2H, OCH_2), 3.97 (s, 3H, OCH_3), 3.94 (s, 3H, OCH_3), 3.86 (d, J = 4.4 Hz, 4H, $CH_2 \times 2$), 3.71 (d, J = 4.4 Hz, 4H, $CH_2 \times 2$). ^{13}C NMR (DMSO-d_6): δ 168.2 (Cq), 163.7 (Cq), 158.8 (Cq), 156.7 (Cq), 155.0 (Cq), 149.6 (Cq), 148.8 (Cq), 140.3 (Cq), 137.4 (Cq), 136.4 (Cq), 129.0 (CH × 2), 128.4 (CH), 128.2 (CH × 2), 120.2 (CH), 117.0 (CH), 115.5 (CH), 109.8 (Cq), 108.1 (CH), 103.8 (CH_2), 70.0(CH_2), 65.5 ($CH_2 \times 2$),

56.4 (CH_3), 56.1 (CH_3), 49.6 ($CH_2 \times 2$). MS (ESI, *m/z*): 501.1 $[M + H]^+$. ESI-HRMS *m/z*: calc'd for $C_{28}H_{29}N_4O_5$ $[M + H]^+$: 501.2138; found 501.2132.

*4.1.2.6. 2-(benzyloxy)-5-(6,7-dimethoxy-4-morpholinoquinazolin-2-yl)benzamide (**T6**).* White solid; Yield 67.9%; mp 228–230 °C; ^1H NMR (DMSO-d_6): δ 8.90 (d, J = 2.4 Hz, 1H, Ar–H), 8.51 (m, 1H, Ar–H), 7.68 (s, 1H, CONH), 7,63 (s, 1H, CONH), 7.55 (d, J = 7.2 Hz, 2H, Ar–H × 2), 7.37 (m, 3H, Ar–H × 3), 7.17 (s, 1H, Ar–H), 5.34 (s, 2H, OCH_2), 3.97 (s, 3H, OCH_3), 3.93 (s, 3H, OCH_3), 3.86 (m, 4H, $CH_2 \times 2$), 3.70 (d, J = 4.4 Hz, 4H, $CH_2 \times 2$). ^{13}C NMR (DMSO-d_6): δ 166.3 (Cq), 163.1 (Cq), 157.3 (Cq), 156.2 (Cq), 154.3 (Cq), 149.1 (Cq), 147.8 (Cq), 136.2 (Cq), 131.2 (Cq), 130.7 (CH), 130.0 (CH), 128.4 (CH × 2), 127.9 (CH), 127.6 (CH × 2), 123.3 (Cq), 113.0 (CH), 108.8 (CH), 107.3 (Cq), 103.1 (CH), 70.0 (CH_2), 65.8 ($CH_2 \times 2$), 55.7 (CH_3), 55.5 (CH_3), 49.6 ($CH_2 \times 2$). MS (ESI, *m/z*): 501.1$[M + H]^+$. ESI-HRMS *m/z*: calc'd for $C_{28}H_{29}N_4O_5$ $[M + H]^+$: 501.2138; found 501.2132.

*4.1.2.7. 3-(6,7-Dimethoxy-4-morpholinoquinazolin-2-yl)-5-(trifluoromethyl)benzamide(**T9**).* White solid; Yield 43.8%; mp 243–245 °C; ^1H NMR (DMSO-d_6): δ 9.19 (s, 1H, Ar–H), 8.84 (s, 1H, Ar–H), 8.40 (s, 1H, CONH), 8.32 (s, 1H, Ar–H), 7.73 (s, 1H, CONH), 7.42 (s, 1H, Ar–H), 7.20 (s, 1H, Ar–H), 3.98 (s, 3H, OCH_3), 3.95 (s, 3H, OCH_3), 3.87 (d, J = 4.4 Hz, 4H, $CH_2 \times 2$), 3.76 (d, J = 4.0 Hz, 4H, $CH_2 \times 2$). ^{13}C NMR (DMSO-d_6): δ 166.9 (Cq), 163.8 (Cq), 155.4 (Cq), 149.4 (Cq), 149.0 (Cq), 140.2 (Cq), 136.3 (Cq), 131.0 (CH), 130.0 (Cq), 129.7 (CH), 126.6 (Cq), 125.5 (CH), 124.5 (Cq, $J_{C\text{-}F}$ = 271 Hz), 110.0 (Cq), 108.14 (CH), 103.8 (CH), 66.4 ($CH_2 \times 2$), 56.5 (CH_3), 56.2 (CH_3), 50.2($CH_2 \times 2$). MS (ESI, *m/z*): 463.1 $[M + H]^+$. ESI-HRMS *m/z*: calc'd for $C_{22}H_{22}F_3N_4O_4$ $[M + H]^+$: 463.1593; found 463.1588.

*4.1.2.8. 3-(6,7-Dimethoxy-4-morpholinoquinazolin-2-yl)-5-(trifluoromethoxy) benzamide (**T10**).* White solid; Yield 57.3%; mp 222–224 °C; ^1H NMR (DMSO-d_6): δ 8.96 (s, 1H, Ar–H), 8.47 (s, 1H, Ar–H), 8.31 (s, 1H, Ar–H), 7.94 (s, 1H, CONH), 7.69 (s, 1H, CONH), 7.39 (s, 1H, Ar–H), 7.15 (s, 1H, Ar–H), 3.98 (s, 3H, OCH_3), 3.95 (s, 3H, OCH_3), 3.86 (d, J = 4.4 Hz, 4H, $CH_2 \times 2$), 3.76 (d, J = 4.0 Hz, 4H, $CH_2 \times 2$). ^{13}C NMR (DMSO-d_6): 166.8 (Cq), 163.8 (Cq), 155.4 (Cq), 155.1 (Cq), 149.4 (Cq), 149.0 (Cq), 141.4 (Cq), 137.3 (Cq), 126.1 (Cq), 122.4 (Cq), 121.9 (CH), 120.6 (CH), 119.4 (CH), 108.1 (CH), 103.8 (CH), 66.4 ($CH_2 \times 2$), 56.4 (CH_3), 56.1 (CH_3), 50.2 ($CH_2 \times 2$). MS (ESI, *m/z*): 479.1 $[M + H]^+$. ESI-HRMS *m/z*: calc'd for $C_{22}H_{22}F_3N_4O_5$ $[M + H]^+$: 479.1542; found 479.1537.

*4.1.2.9. Methyl 3-(6, 7-dimethoxy-4-morpholinoquinazolin-2-yl) benzoate (**T12**).* White solid; Yield 77.8%; mp 207–209 °C; ^1H NMR (DMSO-d_6): δ 9.08 (s, 1H, Ar–H), 8.71 (d, J = 8.0 Hz, 1H, Ar–H), 7.66 (d, J = 8.0 Hz, 1H, Ar–H), 7.67 (m, 1H, Ar–H), 7.38 (s, 1H, Ar–H), 7.18 (s, 1H, Ar–H), 3.99 (s, 3H, OCH_3), 3.94 (s, 3H, OCH_3), 3.93 (s, 3H, OCH_3), 3.87 (m, 4H, $CH_2 \times 2$), 3.74 (d, J = 4.4 Hz, 4H, $CH_2 \times 2$). ^{13}C NMR (DMSO-d_6): δ 168.7 (Cq), 163.8 (Cq), 156.4 (Cq), 155.0 (Cq), 149.6 (Cq), 148.8 (Cq), 139.3 (Cq), 132.6 (CH), 130.9 (Cq), 130.4 (CH), 129.5 (CH), 128.6 (CH), 109.9 (Cq), 108.1 (CH), 103.8 (CH), 66.5 (2C), 56.5 (CH_3), 56.2 (CH_3), 52.8 (CH_3), 50.3 ($CH_2 \times 2$). MS (ESI, *m/z*): 410.1 $[M + H]^+$. ESI-HRMS *m/z*: calc'd for $C_{22}H_{24}N_3O_5$ $[M + H]^+$: 410.1716; found 410.1717.

*4.1.2.10. 3-(6, 7-dimethoxy-4-morpholinoquinazolin-2-yl)-N-methylbenzamide (**T14**).* Off-white solid; Yield 43.5%; mp 220–221 °C; ^1H NMR (DMSO-d_6): δ 8.91 (s, 1H, Ar–H), 8.59 (m, 2H, Ar–H × 2), 7.91 (d, J = 8.0 Hz, 1H, Ar–H), 7.59 (m, 1H, CONH), 7.37 (s, 1H, Ar–H), 7.19 (s, 1H, Ar–H), 3.98 (s, 3H, OCH_3), 3.95 (s, 3H, OCH_3), 3.87 (m, 4H, $CH_2 \times 2$), 3.74 (d, J = 4.4 Hz, 4H, $CH_2 \times 2$), 2.84 (d, J = 4.8 Hz, 3H, NH_3). ^{13}C NMR (DMSO-d_6): δ 167.2 (Cq), 163.8 (Cq), 157.0 (Cq), 155.0 (Cq), 149.6 (Cq), 148.7 (Cq), 139.0 (Cq), 135.5 (Cq), 130.5 (CH), 128.8 (CH), 128.7 (CH), 127.0 (CH), 109.8 (Cq), 108.0 (CH), 103.8 (CH), 66.5 ($CH_2 \times 2$), 56.4 (CH_3), 56.2 (CH_3), 50.3 (2C), 26.8 (CH_3). MS (ESI, *m/z*): 409.1 $[M + H]^+$. ESI-HRMS *m/z*: calc'd for $C_{22}H_{25}N_4O_4$ $[M + H]^+$: 409.1876; found 409.1871.

*4.1.2.11. 3-(6,7-Dimethoxy-4-morpholinoquinazolin-2-yl)-N,N-dimethylbenzamide (**T15**).* Off-white solid; Yield 64.6%; mp 169–171 °C; ^1H NMR (DMSO-d_6): δ 8.52 (d, J = 7.6 Hz, 1H, Ar–H), 8.46 (s, 1H, Ar–H), 7.58 (m, 1H, Ar–H), 7.51 (d, J = 7.6 Hz, 1H, Ar–H), 7.35 (s, 1H, Ar–H), 7.19 (s, 1H, Ar–H), 3.97 (s, 3H, OCH_3), 3.95 (s, 3H, OCH_3), 3.86 (m, 4H, $CH_2 \times 2$), 3.72 (d, J = 4.4 Hz, 4H, $CH_2 \times 2$), 3.04 (s, 3H, NH_3), 2.97 (s, 3H, NH_3). ^{13}C NMR (DMSO-d_6): δ 170.6 (Cq), 163.8 (Cq), 156.8 (Cq), 155.0 (Cq), 149.6 (Cq), 148.7 (Cq), 138.8 (Cq), 137.1 (Cq), 128.9 (CH), 128.8 (CH), 128.7 (CH), 126.5 (CH), 109.8 (Cq), 108.1 (CH), 103.8 (CH), 66.5 ($CH_2 \times 2$), 56.4 (CH_3), 56.1 (CH_3), 50.3 ($CH_2 \times 2$), 35.2 ($CH_3 \times 2$). MS (ESI, *m/z*): 423.1 $[M + H]^+$. ESI-HRMS *m/z*: calc'd for $C_{22}H_{27}N_4O_4$ $[M + H]^+$: 423.2032; found 423.2027.

*4.1.2.12. N-(3-(6,7-Dimethoxy-4-morpholinoquinazolin-2-yl)phenyl) acetamide (**T16**).* Off-white solid; Yield 47.8%; mp 228–230 °C; ^1H NMR (DMSO-d_6): δ 10.10 (s, 1H, CONH), 8.60 (s, 1H, Ar–H), 8.14 (d, J = 8.0 Hz, 1H, Ar–H), 7.80 (m, 1H, Ar–H), 7.41 (d, 1H, Ar–H), 7.28 (s, 1H, Ar–H), 7.18 (s, 1H, Ar–H), 3.98 (s, 3H, OCH_3), 3.94 (s, 3H, OCH_3), 3.86 (s, 4H, $CH_2 \times 2$), 3.71 (s, 4H, $CH_2 \times 2$), 2.09 (s, 3H, $COCH_3$). ^{13}C NMR (DMSO-d_6): δ 168.9 (Cq), 163.7 (Cq), 157.4 (Cq), 154.9 (Cq), 149.6 (Cq), 148.6 (Cq), 139.9 (Cq), 139.3 (Cq), 129.1 (CH), 122.9 (CH), 121.0 (CH), 118.9 (CH), 109.7 (Cq), 107.9 (CH), 103.8 (CH), 66.5 ($CH_2 \times 2$), 56.3 (CH_3), 56.1 (CH_3), 50.3 ($CH_2 \times 2$), 24.5 (CH_3). MS (ESI, *m/z*): 409.1 $[M + H]^+$. ESI-HRMS *m/z*: calc'd for $C_{22}H_{25}N_4O_4$ $[M + H]^+$: 409.1876; found 409.1870.

*4.1.2.13. 4-(6, 7-dimethoxy-4-morpholinoquinazolin-2-yl)benzamide (**T17**).* Off-white solid; Yield 78.3%; mp 251–253 °C; ^1H NMR (DMSO-d_6): δ 8.51 (d, J = 8.4 Hz, 2H, Ar–H × 2), 8.08 (s, 1H, CONH), 8.00 (d, J = 8.4 Hz, 2H, Ar–H × 2), 7.46 (s, 1H, CONH), 7.35 (s, 1H, Ar–H), 7.19 (s, 1H, Ar–H), 3.98 (s, 3H, OCH_3), 3.95 (s, 3H, OCH_3), 3.86 (d, J = 4.4 Hz, 4H, $CH_2 \times 2$), 3.74 (d, J = 4.4 Hz, 4H, $CH_2 \times 2$). ^{13}C NMR (DMSO-d_6): δ 168.1 (Cq), 163.7 (Cq), 156.7 (Cq), 155.0 (Cq), 149.6 (Cq), 148.8 (Cq), 141.3 (Cq), 135.8 (Cq), 128.1 (CH × 2), 127.8 (CH × 2), 109.0 (Cq), 108.1 (CH), 103.8 (CH), 66.5 ($CH_2 \times 2$), 56.3 (CH_3), 56.1 (CH_3), 50.3 ($CH_2 \times 2$). MS (ESI, *m/z*): 395.1 $[M + H]^+$. ESI-HRMS *m/z*: calc'd for $C_{21}H_{23}N_4O_4$ $[M + H]^+$: 395.1719; found 395.1714.

*4.1.2.14. N-(4-(6,7-Dimethoxy-4-morpholinoquinazolin-2-yl)phenyl) acetamide (**T18**).* Off-white solid; Yield 57.4%; mp 244–246 °C; ^1H NMR (DMSO-d_6): δ 10.14 (s, 1H, NH), 8.39 (d, J = 8.8 Hz, 2H, Ar–H × 2), 7.72 (d, J = 8.4 Hz, 2H, Ar–H × 2), 7.26 (s, 1H, Ar–H), 7.16 (s, 1H, Ar–H), 3.97 (s, 3H, OCH_3), 3.93 (s, 3H, OCH_3), 3.85 (d, J = 4.4 Hz, 4H, $CH_2 \times 2$), 3.70 (d, J = 4.4 Hz, 4H, $CH_2 \times 2$), 2.09 (s, 3H, $COCH_3$). ^{13}C NMR (DMSO-d_6): δ 168.1 (Cq), 163.7 (Cq), 157.2 (Cq), 154.9 (Cq), 149.7 (Cq), 148.4 (Cq), 141.4 (Cq), 133.3 (Cq), 128.7 (CH × 2), 118.9 (CH × 2), 109.5 (Cq), 107.9 (CH), 103.8 (CH), 66.5 ($CH_2 \times 2$), 56.3 (CH_3), 56.1 (CH_3), 50.3 ($CH_2 \times 2$), 24.6 (CH_3). MS (ESI, *m/z*): 409.1 $[M + H]^+$. ESI-HRMS *m/z*: calc'd for $C_{22}H_{25}N_4O_4$ $[M + H]^+$: 409.1876; found 409.1871.

*4.1.2.15. 3-Methoxy-5-(7-methoxy-6-(2-methoxyethoxy)-4-morpholinoquinazolin-2-yl) benzamide (**T19**).* White solid; Yield 62.1%; mp 209–211 °C; ^1H NMR (DMSO-d_6): δ 8.55 (s, 1H, Ar–H), 8.13 (m, 2H, Ar–H, CONH), 7.54 (m, 1H, Ar–H), 7.46 (s, 1H, CONH), 7.37 (s, 1H, Ar–H), 7.23 (s, 1H, Ar–H), 4.28 (m, 2H, CH_2), 3.98 (s, 3H, OCH_3), 3.90 (s, 3H, OCH_3), 3.86 (d, J = 4.4 Hz, 4H, $CH_2 \times 2$), 3.74 (m, 6H, $CH_2 \times 3$), 3.35 (s, 3H, OCH_3). ^{13}C NMR (DMSO-d_6): δ 168.3 (Cq), 163.8 (Cq), 159.7 (Cq), 156.8 (Cq), 155.0 (Cq), 149.6 (Cq), 148.0 (Cq), 140.3 (Cq), 136.4 (Cq), 120.0 (CH), 116.2 (CH), 114.5 (CH), 109.8 (Cq),

108.1 (CH), 104.9 (CH), 70.8 (CH_2), 68.3 (CH_2), 66.5 ($CH_2 \times 2$), 58.7 (CH_3), 56.4 (CH_3), 55.9 (CH_3), 50.3 ($CH_2 \times 2$). MS (ESI, *m/z*): 469.0 $[M + H]^+$. ESI-HRMS *m/z*: calc'd for $C_{24}H_{29}N_4O_6$ $[M + H]^+$: 469.2087; found 469.2082.

*4.1.2.16. 3-(6,7-Bis(2-methoxyethoxy)-4-morpholinoquinazolin-2-yl)-5-methoxybenzamide(**T20**).* White solid; Yield 63.1%; mp 124–126 °C; ^{1}H NMR (DMSO-d_6): δ 8.54 (s, 1H, Ar–H), 8.12 (s, 2H, Ar–H, CONH), 7.53 (s, 1H, Ar–H), 7.46 (s, 1H, CONH), 7.38 (s, 1H, Ar–H), 7.26 (s, 1H, Ar–H), 4.32 (m, 4H, CH_2), 3.90 (s, 3H, OCH_3), 3.86 (d, J = 4.4 Hz, 4H, $CH_2 \times 2$), 3.75 (m, 4H, $CH_2 \times 2$), 3.37 (s, 6H, $OCH_3 \times 2$). ^{13}C NMR (DMSO-d_6): δ 168.3 (Cq), 163.8 (Cq), 159.7 (Cq), 156.8 (Cq), 154.3 (Cq), 149.5 (Cq), 148.0 (Cq), 140.3 (Cq), 136.4 (Cq), 120.0 (CH), 116.3 (CH), 114.4 (CH), 109.8 (Cq), 108.9 (CH), 105.5 (CH), 70.9 (CH_2), 70.5 (CH_2), 68.7 (CH_2), 68.6 (CH_2), 66.5 ($CH_2 \times 2$), 58.9 (CH_3), 58.8 (CH_3), 55.9 (CH_3), 50.3 ($CH_2 \times 2$). MS (ESI, *m/z*): 513.2 $[M + H]^+$. ESI-HRMS *m/z*: calc'd for $C_{26}H_{33}N_4O_7$ $[M + H]^+$: 513.2349; found 513.2350.

*4.1.2.17. 3-(7-(benzyloxy)-6-methoxy-4-morpholinoquinazolin-2-yl)-5-methoxybenzamide (**T21**).* White solid; Yield 83.2%; mp 240–242 °C; ^{1}H NMR (DMSO-d_6): δ 8.54 (s, 1H, Ar–H), 8.12 (m, 2H, Ar–H, CONH), 7.53 (d, J = 7.2 Hz, 3H, Ar–H × 3), 7.46 (m, 4H, CONH, Ar–H × 3), 7.38 (s, 1H, Ar–H), 7.19 (s, 1H, Ar–H), 5.34 (s, 2H, OCH_2), 4.32 (m, 2H, CH_2), 3.95 (s, 3H, OCH_3), 3.90 (s, 3H, OCH_3), 3.87 (m, 4H, $CH_2 \times 2$), 3.74 (d, J = 4.4 Hz, 4H, $CH_2 \times 2$). ^{13}C NMR (DMSO-d_6): δ 168.3 (Cq), 163.8 (Cq), 159.7 (Cq), 156.8 (Cq), 153.9 (Cq), 149.5 (Cq), 148.9 (Cq), 140.3 (Cq), 136.8 (Cq), 136.5 (Cq), 129.0 (CH × 2), 128.6 (CH), 128.4 (CH × 2), 120.0 (Cq), 116.3 (CH), 114.4 (CH), 109.9 (Cq), 109.3 (CH), 104.1 (CH), 70.5 (CH_2), 66.5 ($CH_2 \times 2$), 56.2 (CH_3), 55.9 (CH_3), 50.2 ($CH_2 \times 2$). MS (ESI, *m/z*): 501.1 $[M + H]^+$. ESI-HRMS *m/z*: calc'd for $C_{28}H_{29}N_4O_5$ $[M + H]^+$: 501.2138; found 501.2132.

*4.1.2.18. 5-(6,7-Dimethoxy-4-morpholinoquinazolin-2-yl)-2-yl)pyrimidin-2-amine (**T11**).* Compound **T11** was synthesized from 5-bromopyrimidin-2-amine (0.05 g, 0.13 mmol) using the general procedure described above. Off-white solid; Yield 67.8%; mp > 250 °C; ^{1}H NMR (DMSO-d_6): δ 9.16 (s, 2H, Ar–H × 2), 7.25 (s, 1H, Ar–H), 7.14 (s, 1H, Ar–H), 7.10 (s, 2H, NH_2), 3.95 (s, 3H, OCH_3), 3.92 (s, 3H, OCH_3), 3.86 (d, J = 4.4 Hz, 4H, $CH_2 \times 2$), 3.69 (d, J = 4.0 Hz, 4H, $CH_2 \times 2$). ^{13}C NMR (DMSO-d_6): δ 164.5 (Cq), 163.6 (Cq), 158.2 (CH × 2), 155.4 (Cq), 154.9 (Cq), 149.6 (Cq), 148.2 (Cq), 120.8 (Cq), 109.4 (Cq), 107.7 (CH), 103.9 (CH), 66.4 ($CH_2 \times 2$), 56.3 (CH_3), 56.1 (CH_3), 50.2 ($CH_2 \times 2$). MS (ESI, *m/z*): 369.1 $[M + H]^+$. ESI-HRMS *m/z*: calc'd for $C_{18}H_{21}N_6O_3$ $[M + H]^+$: 369.1675; found 369.1670.

*4.1.3. General procedure for the synthesis of compounds **T7** and **T8***

To the solution of compound **T5** or **T6** (0.4 mmol) in the mixture of DMF (6 mL) and water (3 mL) was added ammonium formate (0.25 g, 4 mmol) and 5% Pd on carbon (0.1 mmol) and the above mixture was stirred at 100 °C for 6 h. The mixture was filtered and the filtrate was evaporated under vacuum to give a residue. The residue was dissolved in 10 mL water. The water suspension was extracted with ethyl acetate (10 mL × 3). The combined organic extracts was washed by saturated sodium chloride, dried, filtered and evaporated under vacuum to afford compounds **T7**–**T8**.

*4.1.3.1. 3-(6,7-Dimethoxy-4-morpholinoquinazolin-2-yl)-5-hydroxybenzamide (**T7**).* White solid; Yield 84.7%; mp 238–240 °C; ^{1}H NMR (DMSO-d_6): δ 9.77 (s, 1H, Ar–H), 8.39 (s, 1H, Ar–H), 8.05 (s, 1H, CONH), 8.00 (s, 1H, CONH), 7.33 (s, 3H, Ar–H × 2, OH), 7.19 (s, 1H, Ar–H), 3.98 (s, 3H, OCH_3), 3.94 (s, 3H, OCH_3), 3.87 (d, 4H, J = 4.4 Hz, $CH_2 \times 2$), 3.82 (d, 4H, J = 4.0 Hz, $CH_2 \times 2$). ^{13}C NMR (DMSO-d_6): δ 168.7 (Cq), 163.8 (Cq), 157.8 (Cq), 157.1 (Cq), 154.9 (Cq), 149.6 (Cq), 148.7 (Cq), 140.2 (Cq), 135.6 (Cq), 118.4 (CH), 117.6 (CH), 116.4 (CH), 109.8 (Cq), 108.0 (CH), 103.8 (CH), 66.5 ($CH_2 \times 2$), 56.4 (CH_3), 56.1 (CH_3), 50.3 ($CH_2 \times 2$). MS (ESI, *m/z*): 425.1 $[M + H]^+$. ESI-HRMS *m/z*: calc'd for $C_{21}H_{23}N_4O_5$ $[M + H]^+$: 411.1668; found 411.1663.

*4.1.3.2. 5-(6,7-Dimethoxy-4-morpholinoquinazolin-2-yl)-2-hydroxybenzamide (**T8**).* White solid; Yield 81.8%; mp > 250 °C; ^{1}H NMR (DMSO-d_6): δ 9.77 (s, 1H, Ar–H), 8.39 (s, 1H, Ar–H), 8.05 (s, 1H, CONH), 8.00 (s, 1H, CONH), 7.33 (s, 3H, Ar–H × 2, OH), 7.19 (s, 1H, Ar–H), 3.98 (s, 3H, OCH_3), 3.94 (s, 3H, OCH_3), 3.87 (d, J = 4.4 Hz, 4H, $CH_2 \times 2$), 3.82 (s, J = 4.0 Hz, 4H, $CH_2 \times 2$). ^{13}C NMR (DMSO-d_6): δ 172.1 (Cq), 163.7 (Cq), 163.6 (Cq), 162.8 (Cq), 157.0 (Cq), 154.9 (Cq), 148.3 (Cq), 133.8 (CH), 128.6 (CH), 124.6 (CH), 117.8 (Cq), 115.3 (Cq), 109.2 (Cq), 107.6 (CH), 103.9 (CH), 66.5 ($CH_2 \times 2$), 56.3 (CH_3), 56.1 (CH_3), 50.3 ($CH_2 \times 2$). MS (ESI, *m/z*): 411.1 $[M + H]^+$. ESI-HRMS *m/z*: calc'd for $C_{21}H_{23}N_4O_5$ $[M + H]^+$: 411.1668; found 411.1663.

*4.1.4. 3-(6,7-Dimethoxy-4-morpholinoquinazolin-2-yl)benzoic acid (**T13**)*

To a solution of compound **T12** (0.4 mmol) in the mixture of methanol (10 mL) and water (8 mL) was added 2 M NaOH (2 mL, 4 mmol) and the mixture was stirred at room temperature for 4 h. The solvent was removed and 20 mL water was added to the mixture. The suspension was adjusted to pH 4–5 with 6 M hydrochloric acid whereupon a white precipitate formed. The suspension was filtered and dried to give a Off-white solid; Yield 85.4%; mp > 250 °C; ^{1}H NMR (DMSO-d_6): δ 8.92 (s, 1H, Ar–H), 8.69 (d, J = 7.6 Hz, 1H, Ar–H), 8.21 (d, J = 7.6 Hz, 1H, Ar–H), 7.77 (m, 1H, Ar–H), 7.72 (s, 1H, Ar–H), 7.36 (s, 1H, Ar–H), 4.15 (s, 4H, $CH_2 \times 2$), 4.00 (s, 3H, OCH_3), 3.97 (s, 3H, OCH_3), 3.85 (d, J = 4.0 Hz, 4H, $CH_2 \times 2$). ^{13}C NMR (DMSO-d_6): δ 167.1 (Cq × 2), 163.8 (Cq), 156.0 (Cq), 153.3 (Cq), 148.7 (Cq × 2), 133.5 (Cq), 133.4 (CH), 132.0 (CH), 129.8 (CH), 126.7 (CH), 109.9 (Cq), 105.9 (CH), 103.7 (CH), 66.4 ($CH_2 \times 2$), 56.8 (CH_3), 56.5 (CH_3), 49.8 ($CH_2 \times 2$). MS (ESI, *m/z*): 396.1 $[M + H]^+$. ESI-HRMS *m/z*: calc'd for $C_{21}H_2N_3O_5$ $[M + H]^+$:396.1559; found 396.1554.

*4.1.5. 3-(7-Hydroxy-6-methoxy-4-morpholinoquinazolin-2yl)-5-methoxybenzamide (**5**)*

Compound **5** was prepared from compound **T21** as the same procedure with **T7**. White solid; Yield 84.5%; mp 236–237 °C; ^{1}H NMR (DMSO-d_6): δ 10.53 (bm, 1H, OH), 8.50 (s, 1H, Ar–H), 8.10 (m, 2H, Ar–H, CONH),7.52 (m, 1H, Ar–H), 7.45 (s, 1H, CONH), 7.21 (s, 1H, Ar–H), 7.18 (s, 1H, Ar–H), 3.95 (s, 3H, OCH_3), 3.89 (s, 3H, OCH_3), 3.86 (d, J = 4.4 Hz, 4H, $CH_2 \times 2$), 3.71 (d, J = 4.4 Hz, 4H, $CH_2 \times 2$). MS (ESI, *m/z*): 411.1 $[M + H]^+$.

*4.1.6. General procedure for the synthesis of compounds **6** and **T22**–**T26***

To the solution of compound **5** (1 mmol) in DMF (5 mL) was added potassium carbonate (0.55 g, 4 mmol) and the mixture was stirred at room temperature for 10 min. Then alkyl halides (2 mmol) and potassium iodide (0.17 g, 0.1 mmol) was added to the above mixture and the mixture was stirred at 90 °C for 5-8 h under nitrogen atmosphere. The solvent was removed under vacuum and the residue was suspended in water. The suspension was extracted by dichloromethane (10 mL × 3) and the combined organic layer was evaporated under reduced pressure to afford the crude product. The crude product was recrystallized from ethanol to afford compound **6** or **T22**–**T26** as a white or an off-white solid.

*4.1.6.1. Ethyl 2-((2-(3-carbamoyl-5-methoxyphenyl)-6-methoxy-4-morpholinoquinazolin-7-yl)oxy)acetate (**6**).* Off-white solid; Yield

85.2%; mp 199–201 °C; ^{1}H NMR (DMSO-d_6): δ 8.53 (s, 1H, Ar–H), 8.11 (d, J = 1.6 Hz, 2H, Ar–H, CONH), 7.54 (m, 1H, Ar–H), 7.46 (s, 1H, CONH), 7.29 (s, 1H, Ar–H), 7.23 (s, 1H, Ar–H), 5.06 (s, 2H, OCH_2), 4.22 (m, 2H, CH_2), 3.97 (s, 3H, OCH_3), 3.90 (s, 3H, OCH_3), 3.87 (m, 4H, $CH_2 \times 2$), 3.75 (d, J = 2.4 Hz, 4H, $CH_2 \times 2$), 1.25 (t, J_1 = 6.8 Hz, J_2 = 7.2 Hz, 3H, CH_3). MS (ESI, m/z): 497.8 $[M + H]^+$.

*4.1.6.2. 3-Methoxy-5-(6-methoxy-7-(2-methoxyethoxy)-4-morpholinoquinazolin-2-yl) benzamide (**T22**).* White solid; Yield 74.1%; mp 210–212 °C; ^{1}H NMR (DMSO-d_6): δ 8.55 (s, 1H, Ar–H), 8.12 (d, J = 1.2 Hz, 2H, Ar–H, CONH), 7.54 (s, 1H, Ar–H), 7.46 (s, 1H, CONH), 7.38 (s, 1H, Ar–H), 7.19 (s, 1H, Ar–H), 4.32 (m, 2H, CH_2), 3.95 (s, 3H, OCH_3), 3.90 (s, 3H, OCH_3), 3.86 (d, J = 4.4 Hz, 4H, $CH_2 \times 2$), 3.75 (m, 6H, $CH_2 \times 3$), 3.35 (s, 3H, OCH_3). ^{13}C NMR (DMSO-d_6): δ 168.3 (Cq), 163.7 (Cq), 159.7 (Cq), 156.8 (Cq), 154.1 (Cq), 149.5 (Cq), 148.7 (Cq), 140.3 (Cq), 136.4 (Cq), 120.0 (CH), 116.2 (CH), 114.4 (CH), 109.8 (Cq), 108.7 (CH), 103.9 (CH), 70.5 (CH_2), 68.4 (CH_2), 66.5 ($CH_2 \times 2$), 58.7 (CH_3), 56.1 (CH_3), 55.9 (CH_3), 50.3 ($CH_2 \times 2$). MS (ESI, m/z): 469.2 $[M + H]^+$. ESI-HRMS m/z: calc'd for $C_{24}H_{29}N_4O_6$ $[M + H]^+$: 469.2087; found 469.2082.

*4.1.6.3. 3-Methoxy-5-(6-methoxy-4-morpholino-7-((tetrahydro-2H-pyran-4-yl) methoxy)quinazolin-2yl)benzamide (**T23**).* White solid; Yield 67.8%; mp 231–233 °C; ^{1}H NMR (DMSO-d_6): δ 8.55 (s, 1H, Ar–H), 8.12 (m, 2H, Ar–H, CONH), 7.53 (d, J = 1.6 Hz, 1H, Ar–H), 7.45 (s, 1H, CONH), 7.36 (s, 1H, Ar–H), 7.19 (s, 1H, Ar–H), 4.06 (d, J = 6.4 Hz, 2H, CH_2), 3.94 (s, 3H, OCH_3), 3.88 (m, 9H, OCH_3, $CH_2 \times 3$), 3.73 (d, J = 3.6 Hz, 4H, $CH_2 \times 2$), 2.12 (m, 1H, CH), 1.73 (d, J = 12.0 Hz, 2H, CH_2), 1.39 (m, 2H, CH_2). ^{13}C NMR (DMSO-d_6): δ 168.3 (Cq), 163.8 (Cq), 159.7 (Cq), 156.8 (Cq), 154.3 (Cq), 149.6 (Cq), 148.9 (Cq), 140.3 (Cq), 136.4 (Cq), 112.0 (CH), 116.2 (CH), 114.5 (CH), 109.7 (Cq), 108.69 (CH), 103.94 (CH), 73.3 (CH_2), 67.0 ($CH_2 \times 2$), 66.4 ($CH_2 \times 2$), 56.2 (CH_3), 55.9 (CH_3), 50.3 ($CH_2 \times 2$), 34.6 (CH), 29.6 ($CH_2 \times 2$). MS (ESI, m/z): 509.2 $[M + H]^+$. ESI-HRMS m/z: calc'd for $C_{27}H_{33}N_4O_6$ $[M + H]^+$: 509.2400; found 509.2401.

*4.1.6.4. 3-Methoxy-5-(6-methoxy-4-morpholino-7-(2-morpholinoethoxy)quinazolin-2-yl) benzamide (**T24**).* Off-white solid; Yield 69.4%; mp 194–196 °C; ^{1}H NMR (DMSO-d_6): δ 8.54 (s, 1H, Ar–H), 8.12 (m, 2H, Ar–H, CONH), 7.53 (d, J = 1.6 Hz, 1H, Ar–H), 7.45 (s, 1H, CONH), 7.38 (s, 1H, Ar–H), 7.19 (s, 1H, Ar–H), 4.28 (m, 2H, CH_2), 3.94 (s, 3H, OCH_3), 3.90 (s, 3H, OCH_3), 3.86 (d, J = 4.4 Hz, 4H, $CH_2 \times 2$), 3.73 (d, J = 4.0 Hz, 4H, $CH_2 \times 2$), 2.75 (m, 2H, CH_2), 2.48 (s, 4H, $CH_2 \times 2$), 2.79 (m, 4H, $CH_2 \times 2$), 1.52 (m, 4H, $CH_2 \times 2$), 1.40 (m, 2H, CH_2). ^{13}C NMR (DMSO-d_6): δ 168.3 (Cq), 163.7 (Cq), 159.7 (Cq), 156.8 (Cq), 154.1 (Cq), 149.5 (Cq), 148.8 (Cq), 140.3 (Cq), 136.4 (Cq), 120.0 (CH), 116.2 (CH), 114.4 (CH), 109.8 (Cq), 108.8 (CH), 103.9 (CH), 66.9 (CH_2), 66.6 ($CH_2 \times 2$), 66.5 ($CH_2 \times 2$), 57.2 (CH_2), 56.2 (CH_3), 55.9 (CH_3), 54.1 ($CH_2 \times 2$), 50.3 ($CH_2 \times 2$). MS (ESI, m/z): 522.2 $[M + H]^+$. ESI-HRMS m/z: calc'd for $C_{27}H_{34}N_5O_6$ $[M + H]^+$: 524.2509; found 524.2505.

*4.1.6.5. 3-Methoxy-5-(6-methoxy-4-morpholino-7-(2-(piperidin-1-yl)ethoxy) quinazolin-2-yl)benzamide (**T25**).* Off-white solid; Yield 63.1%; mp 192–194 °C; ^{1}H NMR (DMSO-d_6): δ 8.54 (s, 1H, Ar–H), 8.12 (m, 2H, Ar–H, CONH), 7.53 (d, J = 1.6 Hz, 1H, Ar–H), 7.45 (s, 1H, CONH), 7.38 (s, 1H, Ar–H), 7.19 (s, 1H, Ar–H), 4.28 (m, 2H, CH_2), 3.94 (s, 3H, OCH_3), 3.90 (s, 3H, OCH_3), 3.86 (d, J = 4.4 Hz, 4H, $CH_2 \times 2$), 3.73 (d, J = 4.0 Hz, 4H, $CH_2 \times 2$), 2.75 (m, 2H, CH_2), 2.48 (s, 4H, $CH_2 \times 2$), 2.79 (m, 4H, $CH_2 \times 2$), 1.52 (m, 4H, $CH_2 \times 2$), 1.40 (m, 2H, CH_2). ^{13}C NMR (DMSO-d_6): δ 168.3 (Cq), 163.7 (Cq), 159.7 (Cq), 156.8 (Cq), 154.4 (Cq), 149.6 (Cq), 148.8 (Cq), 140.3 (Cq), 136.4 (Cq), 120.0 (CH), 116.2 (CH), 114.5 (CH), 109.8 (Cq), 108.8 (CH), 103.9 (CH), 67.1 (CH_2), 66.5 ($CH_2 \times 2$), 57.6 (CH_2), 56.2 (CH_3), 55.9 (CH_3), 54.9 ($CH_2 \times 2$), 50.26 ($CH_2 \times 2$), 26.04 ($CH_2 \times 2$), 24.40 (CH_2). MS (ESI, m/z): 522.2 $[M + H]^+$. ESI-HRMS m/z: calc'd for $C_{28}H_{36}N_5O_5$ $[M + H]^+$: 522.2716; found 522.2711.

*4.1.6.6. 3-Methoxy-5-(6-methoxy-4-morpholino-7-(2-(pyrrolidin-1-yl)ethoxy) quinazolin-2-yl)benzamide (**T26**).* Off-white solid; Yield 72.7%; mp 195–197 °C; ^{1}H NMR (DMSO-d_6): δ 8.54 (s, 1H, Ar–H), 8.12 (m, 2H, Ar–H, CONH), 7.53 (d, J = 1.6 Hz, 1H, Ar–H), 7.45 (s, 1H, CONH), 7.37 (s, 1H, Ar–H), 7.19 (s, 1H, Ar–H), 4.28 (m, 2H, CH_2), 3.94 (s, 3H, OCH_3), 3.90 (s, 3H, OCH_3), 3.86 (d, J = 4.4 Hz, 4H, $CH_2 \times 2$), 3.73 (d, J = 4.0 Hz, 4H, $CH_2 \times 2$), 2.88 (m, 2H, CH_2), 2.56 (s, 4H, $CH_2 \times 2$), 1.52 (m, 4H, $CH_2 \times 2$), 1.70 (m, 4H, $CH_2 \times 2$). ^{13}C NMR (DMSO-d_6): δ 168.2 (Cq), 163.7 (Cq), 159.7 (Cq), 156.8 (Cq), 153.7 (Cq), 149.5 (Cq), 148.7 (Cq), 140.3 (Cq), 136.4 (Cq), 120.0 (CH), 116.3 (CH), 114.5 (CH), 110.0 (Cq), 109.0 (CH), 104.1 (CH), 66.5 ($CH_2 \times 2$), 56.4 (CH_3), 55.9 (CH_3), 54.6 ($CH_2 \times 3$), 53.9 (CH_2), 50.3 ($CH_2 \times 2$), 23.4 ($CH_2 \times 2$). MS (ESI, m/z): 508.2 $[M + H]^+$. ESI-HRMS m/z: calc'd for $C_{27}H_{34}N_5O_3$ $[M + H]^+$: 508.2560; found 509.2555.

*4.1.7. 2-((2-(3-Carbamoyl-5-methoxyphenyl)-6-methoxy-4-morpholinoquinazolin-7yl)oxy)acetic acid (**7**)*

To a solution of compound **6** (1.00 g, 2 mmol) in the mixture of methanol (12 mL) and water (3 mL) was added 2 M NaOH (10 mL, 20 mmol) and the mixture was stirred at room temperature for 4 h. The solvent was removed and 20 mL water was added to the mixture. The suspension was adjusted to pH 4–5 with 6 M hydrochloric acid whereupon a white precipitate formed. The suspension was filtered and dried to give a white solid. Yield 71.2%; mp > 250 °C; ^{1}H NMR (DMSO-d_6): δ 8.48 (s, 1H, Ar–H), 8.23 (s, 1H, CONH), 8.05 (s, 1H, Ar–H), 7.70 (s, 1H, Ar–H), 7.62 (s, 1H, Ar–H), 7.55 (s, 1H, CONH), 7.38 (s, 1H, Ar–H), 4.96 (s, 2H, OCH_2), 4.14 (s, 4H, $CH_2 \times 2$), 3.99 (s, 3H, OCH_3), 3.94 (s, 3H, OCH_3), 3.85 (d, J = 4.0 Hz, 4H, $CH_2 \times 2$). MS (ESI, m/z): 469.1 $[M + H]^+$.

*4.1.8. General procedure for the synthesis of compounds **T27**–**T29***

A solution of compound **7** (0.24 g, 0.51 mmol) in DMF (8 mL) was added alkyl amine (4 mmol), 1-ethyl-3-(3-dimethylaminopropyl) carbodiimide (0.48 g, 2.5 mmol), *N*-hydroxybenzotrizole (0.41 g, 3 mmol) and the mixture was stirred for 8 h at room temperature under nitrogen atmosphere. The solvent was removed in vacuum and the residue was suspended in water (10 mL). The suspension was extracted by ethyl acetate (10 mL × 3). The combined organic layer was washed by sodium bicarbonate and saturated sodium chloride, dried, filtered and evaporated to afford a crude product, which was recrystallized from ethanol to afford compounds **T27**–**T29** as a white or an off-white solid.

*4.1.8.1. 3-Methoxy-5-(6-methoxy-4-morpholino-7-(2-morpholino-2-oxoethoxy)quinazolin-2-yl)benzamide (**T27**).* Off-white solid; Yield 75.4%; mp 141–143 °C; ^{1}H NMR (DMSO-d_6): δ 8.54 (s, 1H, Ar–H), 8.11 (d, J = 1.2 Hz, 2H, Ar–H, CONH), 7.53 (m, 1H, Ar–H), 7.46 (s, 1H, CONH), 7.32 (s, 1H, Ar–H), 7.21 (s, 1H, Ar–H), 5.13 (s, 2H, OCH_2), 3.96 (s, 3H, OCH_3), 3.90 (s, 3H, OCH_3), 3.86 (d, J = 4.4 Hz, 4H, $CH_2 \times 2$), 3.74 (d, J = 4.4 Hz, 4H, $CH_2 \times 2$), 3.63 (m, 4H, $CH_2 \times 2$). ^{13}C NMR (DMSO-d_6): δ 168.3 (Cq), 165.8 (Cq), 163.7 (Cq), 159.7 (Cq), 156.8 (Cq), 153.7 (Cq), 149.3 (Cq), 148.8 (Cq), 140.3 (Cq), 136.5 (Cq), 120.0 (CH), 116.3 (CH), 114.4 (CH), 110.0 (Cq), 109.3 (CH), 101.1 (CH), 66.6 (CH_2), 66.5 ($CH_2 \times 2$), 56.3 (CH_3), 55.9 (CH_3), 50.3 ($CH_2 \times 2$), 45.2 ($CH_2 \times 2$), 42.1 ($CH_2 \times 2$). MS (ESI, m/z): 538.2 $[M + H]^+$. ESI-HRMS m/z: calc'd for $C_{27}H_{32}N_5O_7$ $[M + H]^+$: 538.2302; found 538.2308.

*4.1.8.2. 3-Methoxy-5-(6-methoxy-7-(2-(4-methylpiperazin-1-yl)-2-oxoethoxy)- 4-morpholinoquinazolin-2-yl)benzamide (**T28**).* Off-white solid; Yield 49.5%; mp 141–143 °C; ^{1}H NMR (DMSO-d_6): δ 8.53 (s, 1H, Ar–H), 8.11 (s, 2H, Ar–H, CONH), 7.53 (d, J = 1.2 Hz, 1H,

Ar–H), 7.45 (s, 1H, CONH), 7.30 (s, 1H, Ar–H), 7.21 (s, 1H, Ar–H), 5.11 (s, 2H, OCH_2), 3.96 (s, 3H, OCH_3), 3.90 (s, 3H, OCH_3), 3.86 (d, $J = 4.4$ Hz, 4H, $CH_2 \times 2$), 3.74 (d, $J = 4.0$ Hz, 4H, $CH_2 \times 2$), 3.50 (s, 4H, $CH_2 \times 2$), 2.39 (s, 2H, CH_2), 2.29 (s, 2H, CH_2), 2.21 (s, 3H, CH_3). ^{13}C NMR (DMSO-d_6): δ 168.3 (Cq), 165.5 (Cq), 163.7 (Cq), 159.7 (Cq), 156.8 (Cq), 153.7 (Cq), 149.3 (Cq), 148.8 (Cq), 140.3 (Cq), 136.5 (Cq), 120.0 (CH), 116.3 (CH), 114.4 (CH), 101.0 (Cq), 109.3 (CH), 101.1 (CH), 66.5 (CH_2), 66.5 ($CH_2 \times 2$), 56.3 (CH_3), 55.9 (CH_3), 55.1 (CH_2), 54.8 (CH_2), 50.3 ($CH_2 \times 2$), 46.6 (CH_2), 44.5 (CH_2), 41.7 (CH_2). MS (ESI, *m/z*): 551.2 $[M + H]^+$. ESI-HRMS *m/z*: calc'd for $C_{28}H_{35}N_6O_6$ $[M + H]^+$: 551.2618; found 551.2613.

*4.1.8.3. 3-Methoxy-5-(6-methoxy-7-(2-(mathylamino)-2-oxoethoxy)-4-morpholinoquinazolin-2-yl)benzamide (**T29**).* Off-white solid; Yield 63.7%; mp 193–195 °C; ^1H NMR (DMSO-d_6): δ 8.53 (s, 1H, Ar–H), 8.11 (m, 2H, Ar–H, CONH), 8.05 (m, 1H, NH), 7.53 (d, $J = 1.2$ Hz, 1H, Ar–H), 7.44 (d, $J = 1.6$ Hz, 1H, CONH), 7.25 (s, 1H, Ar–H), 7.22 (s, 1H, Ar–H), 4.73 (s, 2H, OCH_2), 3.97 (s, 3H, OCH_3), 3.90 (s, 3H, OCH_3), 3.87 (m, 4H, $CH_2 \times 2$), 3.75 (d, $J = 4.4$ Hz, 4H, $CH_2 \times 2$), 2.69 (d, $J = 4.8$ Hz, 3H, NCH_3). ^{13}C NMR (DMSO-d_6): δ 168.3 (Cq), 165.5 (Cq), 163.7 (Cq), 159.7 (Cq), 156.8 (Cq), 153.7 (Cq), 149.3 (Cq), 148.8 (Cq), 140.3 (Cq), 136.5 (Cq), 120.0 (CH), 116.3 (CH), 114.4 (CH), 101.0 (Cq), 109.3 (CH), 101.1 (CH), 68.0 (CH), 66.5 ($CH_2 \times 2$), 56.2 (CH_3), 55.9 (CH_3), 50.2 ($CH_2 \times 2$), 26.0 (CH_3). MS (ESI, *m/z*): 482.1 $[M + H]^+$. ESI-HRMS *m/z*: calc'd for $C_{24}H_{28}N_5O_6$ $[M+H]^+$: 482.2040; found 482.2034.

4.2. Biology

4.2.1. Cell culture

The four human tumor cell lines including HCT-116, MCF-7, U-87 MG and A549 were grown as a monolayer respectively. HCT-116, MCF-7 and U-87 MG were maintained in DMEM medium supplemented with 10% heat inactivated fetal bovine serum (FBS). A549 was maintained in RPMI-1640 medium, with 10% heat inactivated calf serum. All cancer cells were incubated in a humidified atmosphere containing 5% CO_2 at 37 °C.

4.2.2. MTT assay

The *in vitro* antiproliferative activities of compounds were determined by MTT assay. 1500–4000 cells per well were seeded into 96-well plates in 200 μL medium and incubated for 24 h. A series of concentrations of synthesized compounds and GDC0941 were added to the wells with DMSO as vehicle control. The mixture was incubated at 37 °C, with a final concentration of 1% DMSO. After 72 h of incubation, 20 μL of MTT solution (5 mg/mL in PBS) was added to each well and incubated at 37 °C for 4 h. The supernatant of each well was removed and the formed blue formazan crystals were dissolved in 200 μL of DMSO. The optical density at 490 nm wavelength was determined by Varioskan Flash Multimode Reader (Thermo scientific). Three separate experiments with triplicate data were performed to obtain mean cell viability. The IC_{50} value, that is, the concentration (μM) of a compound was able to cause 50% cell death with respect to the control culture, were calculated by means of PRISM 5, Graph Pad software.

4.2.3. Hoechst staining

HCT-116 cell line was selected for Hoechst staining assay. 15,000 cells per well were seeded into 96-well plates and incubated for 24 h. The medium was replaced and cells were incubated with compound **T10** at concentrations of 0.1, 1 and 10 μM for 24 h. The controls were treated with vehicle (0.5% DMSO). Before staining, the cells were examined directly and photographed under a phase contrast microscope. Then the cells were treated with Hoechst 33258 for 0.5 h at 37 °C. After washed by PBS, the cells were captured from randomly selected fields under fluorescent microscope to qualitatively determine the morphological changes of HCT-116 cells based on their relative fluorescence and nuclear fragmentation.

4.2.4. Cell cycle analysis

HCT-116 cells were seeded into 6-well plate at a concentration of 3×10^5 cells per well. After 24 h, the medium was replaced and the cells were incubated with compound **T10** at a concentration of 3 μM for 24 h. The controls were treated with vehicle (0.5% DMSO). The cells were then harvested and fixed with 70% ice-cold ethanol overnight at −20 °C. After centrifugation, the cell pellets were treated with propidium iodide (5 μg/mL) and RNase A in PBS (100 μg/mL) in PBS for 30 min at room temperature. DNA was observed and analyzed with a flow cytometer. The independent experiment was repeated three times.

4.2.5. Apoptosis analysis

HCT-116 cells were seeded into 12-well plate at a concentration of 1.5×10^5 cells per well and incubated for 24 h. The medium was replaced and the cells were then incubated with compound **T10** at concentrations of 1 μM and 3 μM for 24 h. The controls were treated with vehicle (0.5% DMSO). The cells were harvested and performed with Annexin V-FITC/PI apoptosis detection Kit according to the manufacturer's instruction. Then the cells were analyzed with a flow cytometer (Guava easyCyte).

4.2.6. PI3Ks enzymatic activities assay

Inhibitory PI3Ks enzymatic activities of compounds **T7**, **T10** and **GDC0941** were evaluated according to process described in Ref. [19]. Compounds **T7**, **T10** and GDC0941 were dissolved in DMSO and diluted to a series of concentrations. Different concentrations of compounds were added to the enzyme reaction buffer containing 40 mM Tris–HCl, pH 7.4, 10 mM $MgCl_2$, 0.1 mg/mL BSA, 1 mM DTT, 2.5 μM ATP, PI3K (p110α/p85α, p110β/p85α, p110γ/PIK3R5 or p110δ/p85α) and L-α-phosphatidylinositol. The final reaction volume was 50 μL. After incubation for 40 min at 30 °C, the reaction was terminated by addition of stop solution. The amount of ADP was then detected via luciferase assay. After incubation for 5 min, the luminescence signal was determined by the multimode reader (MD-SpectraMax M5). The signal intensity is proportional to the PI3K activity.

The percentage of inhibition was calculated based on the following equation

$$\%\ \text{inhibition} = [1 - (Lu_{compound} - Lu_{min})/(Lu_{max} - Lu_{min})] \times 100\%,$$

where $Lu_{compound}$ is the signal at a given compound concentration, Lu_{max} is the signal of PI3Ks without compound and Lu_{min} is the signal of background in the absence of enzyme and compound. The IC_{50} values were calculated according to the fit of the dose–response curves by using Graph Pad Prism 5.

4.2.7. Western blot assay

HCT-116 cells were seeded into 12-well plates at 5×10^5 cells per well and incubated at 37 °C for 16 h. The medium was replaced and cells were incubated with compounds **T10** and GDC0941 at 10 μM at 37 °C for 1 h. The controls were added vehicle (0.5% DMSO). The cells were lysed into ice-cold cell lysis buffer and the cell lysates were centrifuged at 12,000 rpm for 20 min at 4 °C. The supernatant was collected and protein concentrations were determined by BCA protein Assay Kit. The protein samples were separated on SDS-PAGE on 10% gels and then transferred onto nitrocellulose membrane. The membranes were blocked in blocking buffer (10% nonfat dry milk/1% Tween 20 in TBS) for 2 h,

incubated with AKT (Cell Signaling Technology) and p-Ser473 AKT (Cell Signaling Technology), washed by TBST and then incubated with Mouse or rabbit horseradish peroxidase-conjugated secondary antibodies. The protein-antibody complexes were detected by chemiluminescence with a GeneGnome5 system (Syngene, UK). Protein bands were quantified using ImageJ software (National Institutes of Health, Bethesda, MD, USA). β-Actin (Santa Cruz) as a loading control.

4.2.8. *In vivo antitumor effect on established mice S180 homograft models*

Mice (19.6 ± 1.9 g) were purchased from Experiment Animal Center of Xi'an Jiaotong University Health Science Center and fed in the same place. The experimental protocol was approved by Ethic Committee of Xi'an Jiaotong University.

3×10^6 S180 cells were injected subcutaneously into the flank of the mice. All tumor-bearing mice were randomly divided into three groups, with 8 mice in each group. The next day, compound **T10** was dissolved in NMP/PEG400/H_2O (1:8:1) and dosed orally at 15 mg/kg and 30 mg/kg for the low and high dosage groups once a day for 8 days, respectively. In the solvent group, the same volume of solvent was administered orally. Body weights were recorded per day. The mice were anesthetized and sacrificed on Day 9. The weights of the body and the neoplasm were measured and inhibitory ratios of tumor weight were calculated.

4.3. Molecule docking

The protein-ligand complex crystal structure compound **1f** with PI3Kγ [37] was chosen as the template to elucidate the docking mode of **T7** and **T10** with PI3Kγ. Protein structure was downloaded from Protein Data Bank (PDB ID 3R7R) and the C-DOCKER protocol within Discovery Studio 2.5 was used for molecular docking. The PI3Kγ enzyme was prepared by added hydrogen atoms and then defined as a receptor. The site sphere was selected on the basis of the ligand binding location of compound **1f**, which was replaced by compound **T7** or **T10**. After end of molecular docking, 10 docking poses were scored and selected based on calculated C-DOCKER energy.

4.4. Statistical analysis

The data are reported as mean ± standard deviation (SD) for at least three experiments. Statistical differences were analyzed according to one way ANOVA test wherein the differences were considered to be significant at $P < 0.05$. All statistics were calculated using a statistical program PRISM 5, Graph Pad software.

Acknowledgments

Financial support from the National Natural Science Foundation of China (Grant No. 21072156 and 81402792) is gratefully acknowledged.

References

[1] R.D. Taylor, M. MacCoss, A.D.G. Lawson, Rings in drugs, J. Med. Chem. 57 (2014) 5845–5859.
[2] Y. Zhang, L. Jin, H. Xiang, J. Wu, D. Hu, W. Xue, S. Yang, Synthesis and anticancer activities of 5,6,7-trimethoxy-*N*-phenyl(ethyl)-4-aminoquinazoline derivatives, Eur. J. Med. Chem. 66 (2013) 335–344.
[3] R.A. Smits, M. Adami, E.P. Istyastono, O.P. Zuiderveld, C.M.E. van Dam, F.J.J. de Kanter, A. Jongejan, G. Coruzzi, R. Leurs, I.J.P. de Esch, Synthesis and QSAR of quinazoline sulfonamides as highly potent human histamine H_4 receptor inverse agonists, J. Med. Chem. 53 (2010) 2390–2400.
[4] L.F. Kuyper, D.P. Baccanari, M.L. Jones, R.N. Hunter, R.L. Tansik, S.S. Joyner, C. Boytos, S.K. Rudolph, V. Knick, H.R. Wilson, J.M. Caddell, H.S. Friedman, J.C.W. Comley, J.N. Stables, High-affinity inhibitors of dihydrofolate reductase: antimicrobial and anticancer activities of 7,8-dialkyl -1,3-diaminopyrrolo[3,2-*f*]quinazolines with small molecular size, J. Med. Chem. 39 (1996) 892–903.
[5] P. Verhaeghe, N. Azas, M. Gasquet, S. Hutter, C. Ducros, M. Laget, S. Rault, P. Rathelot, P. Vanelle, Synthesis and antiplasmodial activity of new 4-aryl-2-trichloromethylquinazolines, Bioorg. Med. Chem. Lett. 18 (2008) 396–401.
[6] K.S. Jain, J.B. Bariwal, M.K. Kathiravan, M.S. Phoujdar, R.S. Sahne, B.S. Chauhan, A.K. Shah, M.R. Yadav, Recent advances in selective alpha1-adrenoreceptor antagonists as antihypertensive agents, Bioorg. Med. Chem. 16 (2008) 4759–4800.
[7] C.E. Geyer, J. Forster, D. Lindquist, S. Chan, C.G. Romieu, T. Pienkowski, A. Jagiello-Gruszfeld, J. Crown, A. Chan, B. Kaufman, Lapatinib plus capecitabine for HER2-positive advanced breast cancer, N. Engl. J. Med. 355 (2006) 2733–2743.
[8] M.F. Press, H.J. Lenz, EGFR, HER2 and VEGF pathways, Drugs 67 (2007) 2045–2075.
[9] B. Barlaam, J. Anderton, P. Ballard, R.H. Bradbury, L.F.A. Hennequin, D.M. Hickinson, J.G. Kettle, G. Kirk, T. Klinowska, C. LamberTvan der Brempt, C. Trigwell, J. Vincent, D. Ogilvie, Discovery of AZD8931, an equipotent, reversible inhibitor of signaling by EGFR, HER2, and HER3 receptors, ACS Med. Chem. Lett. 4 (2013) 742–746.
[10] J. Sun, D.-D. Li, J.-R. Li, F. Fang, Q.-R. Du, Y. Qian, H.-L. Zhu, Design, synthesis, biological evaluation, and molecular modeling study of 4-alkoxy quinazoline derivatives as potential VEGFR2 kinase inhibitors, Org. Biomol. Chem. 11 (2013) 7676–7686.
[11] M.M. Vasbinder, B. Aquila, M. Augustin, H. Chen, T. Cheung, D. Cook, L. Drew, B.P. Fauber, S. Glossop, M. Grondine, E. Hennessy, J. Johannes, S. Lee, P. Lyne, M. Mörtl, C. Omer, S. Palakurthi, T. Pontz, J. Read, L. Sha, M. Shen, S. Steinbacher, H. Wang, A. Wu, M. Ye, Discovery and optimization of a novel series of potent mutant B-Raf^{V600E} selective kinase inhibitors, J. Med. Chem. 56 (2013) 1996–2015.
[12] L. Leivers, M. Tallant, J.B. Shotwell, S. Dickerson, M.R. Leivers, O.B. McDonald, J. Gobel, K.L. Creech, S.L. Strum, A. Mathis, S. Rogers, C.B. Moore, J. Botyanszki, Discovery of selective small molecule type III phosphatidylinositol 4-kinase alpha (PI4KIIIα) inhibitors as anti hepatitis C (HCV) agents, J. Med. Chem. 57 (2014) 2091–2106.
[13] J.A. Engelman, J. Luo, L.C. Cantley, The evolution of phosphatidylinositol 3-kinases as regulators of growth and metabolism, Nat. Rev. Genet. 8 (2006) 606–619.
[14] P. Liu, H. Cheng, T.M. Roberts, J. Zhao, Targeting the phosphoinositide 3-kinase pathway in cancer, Nat. Rev. Drug. Discovery 8 (2009) 627–644.
[15] A. Parcellier, L.A. Tintignac, E. Zhuravleva, B.A. Hemmings, PKB and the mitochondria: AKTing on apoptosis, Cell. Signal 20 (2008) 21–30.
[16] Y. Samuels, Z. Wang, A. Bardelli, N. Silliman, J. Ptak, S. Szabo, H. Yan, A. Gazdar, S.M. Powell, G.J. Riggins, J.K. Wilson, S. Markowitz, K.W. Kinzler, B. Vogelstein, V.E. Velculescu, High frequency mutations of the PIK3CA gene in human cancers, Science 304 (2004) 554.
[17] L. Salmena, A. Carracedo, P.P. Pandolfi, Tenets of PTEN tumor suppression, Cell 133 (2008) 403–414.
[18] Q. Liu, C. Thoreen, J.H. Wang, D. Sabatini, N.S. Gray, mTOR mediated anticancer drug discovery, Drug Discovery Today: Ther. Strategies 6 (2009) 47–55.
[19] M.T. Burger, S. Pecchi, A. Wagman, Z.-J. Ni, M. Knapp, T. Hendrickson, G. Atallah, K. Pfister, Y.C. Zhang, S. Bartulis, K. Frazier, S. Ng, A. Smith, J. Verhagen, J. Haznedar, K. Huh, E. Iwanowicz, X.H. Xin, D. Menezes, H. Merritt, I. Lee, M. Wiesmann, S. Kaufman, K. Crawford, M. Chin, D. Bussiere, K. Shoemaker, I. Zaror, S.-M. Maira, C.F. Voliva, Identification of NVP-BKM120 as a potent, selective, orally bioavailable class I PI3 kinase inhibitor for treating cancer, ACS Med. Chem. Lett. 2 (2011) 774–779.
[20] J. Folkes, K. Ahmadi, W.K. Alderton, S. Alix, S.J. Baker, G. Box, I.S. Chuckowree, P.A. Clarke, P. Depledge, S.A. Eccles, L.S. Friedman, A. Hayes, T.C. Hancox, A. Kugendradas, L. Lensun, P. Moore, A.G. Olivero, J. Pang, S. Patel, G.H. Pergl-Wilson, F.I. Raynaud, A. Robson, N. Saghir, L. Salphati, S. Sohal, M.H. Ultsch, M. Valenti, H.J.A. Wallweber, N.C. Wan, C. Wiesmann, P. Workman, Al Zhyvoloup, M.J. Zvelebil, S.J. Shuttleworth, The identification of 2-(1*H*-Indazol-4-yl)-6-(4-methanesulfonyl-piperazin-1-ylmethyl) -4-morpholin-4-yl-thieno[3,2-*d*]pyrimidine (GDC-0941) as a potent, selective, orally bioavailable inhibitor of class I PI3 kinase for the treatment of cancer, J. Med. Chem. 51 (2008) 5522–5532.
[21] G.W. Rewcastle, S.A. Gamage, J.U. Flanagan, R. Frederick, W.A. Denny, B.C. Baguley, P. Kestell, R. Singh, J.D. Kendall, E.S. Marshall, C.L. Lill, W.-J. Lee, S. Kolekar, C.M. Buchanan, S.M.F. Jamieson, P.R. Shepherd, Synthesis and biological evaluation of novel analogues of the pan class I phosphatidylinositol 3-kinase (PI3K) inhibitor 2-(difluoromethyl)-1-[4,6-di(4-morpholinyl)-1,3,5-triazin-2-yl]-1H-benzimidazole (ZSTK474), J. Med. Chem. 54 (2011) 7105–7126.
[22] P. Furet, V. Guagnano, R.A. Fairhurst, P. Imbach-Weese, I. Bruce, M. Knapp, C. Fritsch, F. Blasco, J. Blanz, R. Aichholz, J. Hamon, D. Fabbro, G. Caravatti, Discovery of NVP-BYL719 a potent and selective phosphatidylinositol-3 kinase alpha inhibitor selected for clinical evaluation, Bioorg. Med. Chem. Lett. 23 (2013) 3741–3748.
[23] S.-M. Maira, F. Stauffer, J. Brueggen, P. Furet, C. Schnell, C. Fritsch, S. Brachmann, P. Chene, A.D. Pover, K. Schoemaker, D. Fabbro, D. Gabriel, M. Simonen, L. Murphy, P. Finan, W. Sellers, C. Garcia-Echeverria, Identification and characterization of NVP-BEZ235, a new orally available dual

phosphatidylinositol 3-kinase/mammalian target of rapamycin inhibitor with potent in vivo anticancer activity, Mol. Cancer Ther. 7 (2008) 1851–1863.
[24] S.D. Knight, N.D. Adams, J.L. Burgess, Discovery of GSK2126458, a highly potent inhibitor of PI3K and the mammalian target of rapamycin, ACS Med. Chem. Lett. 1 (2010) 39–43.
[25] D.P. Sutherlin, L. Bao, M. Berry, G. Castanedo, I. Chuckowree, J. Dotson, A. Folks, L. Friedman, R. Goldsmith, J. Gunzner, T. Heffron, J. Lesnick, C. Lewis, S. Mathieu, J. Murray, J. Nonomiya, J. Pang, N. Pegg, W.W. Prior, L. Rouge, L. Salphati, D. Sampath, Q. Tian, V. Tsui, N.C. Wan, S. Wang, B. Wei, C. Wiesmann, P. Wu, B. Zhu, A. Olivero, Discovery of a potent, selective, and orally available class I phosphatidylinositol 3-kinase (PI3K)/mammalian target of rapamycin (mTOR) kinase inhibitor (GDC-0980) for the treatment of cancer, J. Med. Chem. 54 (2011) 7579–7587.
[26] H. Cheng, C. Li, S. Bailey, S.M. Baxi, L. Goulet, L. Guo, J. Hoffman, Y. Jiang, T.O. Johnson, T.W. Johnson, D.R. Knighton, J. Li, K.K.-C. Liu, Z. Liu, A.M. Matthew, M. Walls, A.W. Peter, M. Yin, J. Zhu, M. Zientek, Discovery of the highly potent PI3K/mTOR dual inhibitor PF-04979064 through structure-based drug design, ACS Med. Chem. Lett. 4 (2013) 91–97.
[27] M. Venkatesan, C.M. Dehnhardt, E.D. Santos, Z. Chen, O.D. Santos, S. Ayral-Kaloustian, G. Khafizova, N. Brooijmans, R. Mallon, I. Hollander, L. Feldberg, J. Lucas, K.Yu, J. Gibbons, R.T. Abraham, I. Chaudhary, T.S. Mansour, Bis(morpholino-1,3,5-triazine)derivatives: potent adenosine 5′-triphosphate competitive phosphatidylinositol-3-kinase/mammalian target of rapamycin inhibitors: discovery of compound 26 (PKI-587), a highly efficacious dual inhibitor, J. Med. Chem. 53 (2010) 2636–2645.
[28] P. Wu, Y.Z. Hu, Small molecules targeting phosphoinositide 3-kinases, Med. Chem. Commun. 3 (2012) 1337–1355.
[29] S. Hart, V. Novotny-Diermayr, K.C. Goh, M. Williams, Y.C. Tan, L.C. Ong, A. Cheong, B.K. Ng, C. Amalini, B. Madan, H. Nagaraj, R. Jayaraman, K.M. Pasha, K. Ethirajulu, W.J. Chng, N. Mustafa, B.C. Goh, C. Benes, U. Mcdermott, M. Garnett, B. Dymock, J.M. Wood, VS-5584, a novel and highly selective PI3K/mTOR kinase inhibitor for the treatment of cancer molecular cancer, Mol. Cancer. Ther. 12 (2013) 151–161.
[30] Y.L. Zhao, X. Zhang, Y.Y. Chen, S.Y. Lu, Y.F. Peng, X. Wang, C.L. Guo, A.W. Zhou, J.M. Zhang, Y. Luo, Q.C. Shen, J. Ding, L.H. Meng, J. Zhang, Crystal structures of PI3Kα complexed with PI103 and its derivatives: new directions for inhibitors design, ACS Med. Chem. Lett. 5 (2014) 138–142.
[31] M. Hayakawa, H. Kaizawa, H. Moritomo, T. Koizumi, T. Ohishi, M. Okada, M. Ohta, S.I. Tsukamoto, P. Parker, P. Workman, M. Waterfield, Synthesis and biological evaluation of 4-morpholino-phenylquinazolines and related derivatives as novel PI3 kinase p110α inhibitors, Bioorg. Med. Chem. 14 (2006) 6847–6858.
[32] M. Hayakawa, H. Kaizawa, H. Moritomo, K.I. Kawaguchi, T. Koizumi, M. Yamano, K. Matsuda, M. Okada, M. Ohta, Condensed heteroaryl derivatives, WO0183456(A1), 2001.
[33] T. Shao, J. Wang, J.G. Chen, X.M. Wang, H. Li, Y.P. Li, Y. Li, G.D. Yang, Q.B. Mei, S.Q. Zhang, Discovery of 2-methoxy-3-phenylsulfonamino-5-(quinazolin-6-yl or quinolin-6-yl) benzamides as novel PI3K inhibitors and anticancer agents by bioisostere, Eur. J. Med. Chem. 75 (2014) 96–105.
[34] H. Li, X.M. Wang, J. Wang, T. Shao, Y.P. Li, Q.B. Mei, S.M. Lu, S.Q. Zhang, Combination of 2-methoxy-3-phenylsulfonylaminobenzamide and 2-amino benzothiazole to discover novel anticancer agents, Bioorg. Med. Chem. 22 (2014) 3739–3748.
[35] X.M. Wang, J. Xu, Y.P. Li, H. Li, C.S. Jiang, G.D. Yang, S.M. Lu, S.Q. Zhang, Synthesis and anticancer activity evaluation of a series of [1,2,4]triazolo [1,5-a] pyridinyl pyridines in vitro and in vivo, Eur. J. Med. Chem. 67 (2013) 243–251.
[36] T. Saurat, F. Buron, N. Rodrigues, M.-L. de Tauzia, L. Colliandre, S. Bourg, P. Bonnet, G. Guillaumet, M. Akssira, A. Corlu, C. Guillouzo, P. Berthier, P. Rio, M.-L. Jourdan, H. Benedetti, S. Routier, Design, synthesis, and biological activity of pyridopyrimidine scaffolds as novel PI3K/mTOR dual inhibitors, J. Med. Chem. 57 (2014) 613–631.
[37] S.T. Staben, M. Siu, R. Goldsmith, A.G. Olivero, S. Do, D.J. Burdick, T.P. Heffron, J. Dotson, D.P. Sutherlin, B.Y. Zhu, V. Tsui, H. Le, L. Lee, J. Lesnick, C. Lewis, J.M. Murray, J. Nonomiya, J. Pang, W. W Prior, L. Salphati, L. Rouge, D. Sampath, S. Sideris, C. Wiesmann, P. Wu, Structure-based design of thienobenzoxepin inhibitors of PI3-kinase, Bioorg. Med. Chem. Lett. 21 (2001) 4054–4058.